

Target-enriched DNA sequencing clarifies the identity of name-bearing types of the *Gephyromantis plicifer* complex and reveals a new species of mantellid frog from Madagascar

(Amphibia, Anura)

Miguel Vences, Jörn Köhler, Franco Andreone, Ann-Kristin Craul, Angelica Crottini, Louis du Preez, Michaela Preick, Lois Rancilhac, Mark-Oliver Rödel, Mark D. Scherz, Jeffrey W. Streicher, Michael Hofreiter & Frank Glaw

Vences, M., Köhler, J., Andreone, F., Craul, A.-K., Crottini, A., du Preez, L., Preick, M., Rancilhac, L., Rödel, M.-O., Scherz, M. D., Streicher, J. W., Hofreiter, M. & Glaw, F. 2021. Target-enriched DNA sequencing clarifies the identity of name-bearing types of the *Gephyromantis plicifer* complex and reveals a new species of mantellid frog from Madagascar (Amphibia, Anura). *Spixiana* 44(2): 175–202.

Mantellid frogs of the Madagascar-endemic *Gephyromantis plicifer* complex consist of three nominal species (*G. luteus*, *G. plicifer* and *G. sculpturatus*) as well as several genetically divergent lineages (candidate species), but uncertainties surround the identity of the name-bearing types of all three established nomina. We applied laboratory techniques to isolate archival DNA from the three old, liquid-preserved, name-bearing type specimens and conducted target-enriched DNA sequencing of a fragment of the mitochondrial 16S rRNA gene as basis for the revision of their taxonomy. Along with 16S sequences of 161 fresh samples, sequences of a fragment of the nuclear-encoded Rag-1 gene for 97 of these samples, a multi-gene data set of selected samples, and a comprehensive analysis of available advertisement call recordings, the new data suggest a novel taxonomic hypothesis: (1) The name *G. plicifer* applies to a highland clade of populations from the southern Central East, previously referred to as *Gephyromantis* sp. Ca21, with *G. sculpturatus* as a junior synonym. (2) The name *G. luteus* applies to a widespread clade distributed along most of Madagascar's eastern rainforest band, and more specifically, is assigned to a subclade occurring mostly in coastal regions of the northern Central East and North East. (3) Large-sized specimens from Ranomafana (southern Central East) and Andohahela (South East) previously considered to belong to *G. plicifer* in fact represent a hitherto undescribed species, which we here formally name as *G. pedronoi* sp. nov. The three species are distinguished by very high genetic distances (over 8 % in the 16S gene), an absence of haplotype sharing in Rag-1, as well as morphological and bioacoustic characteristics. Moreover, several infra-specific clades with 16S divergences >4 % may represent distinct species, especially within the widespread *G. luteus*, but cannot be unambiguously delimited by available data. We suggest dedicated sampling at contact zones and more extensive bioacoustic study of genotyped call vouchers to clarify their taxonomic status.

Miguel Vences, Ann-Kristin Craul & Lois Rancilhac, Zoologisches Institut, Technische Universität Braunschweig, Mendelssohnstr. 4, 38106 Braunschweig, Germany

Jörn Köhler, Hessisches Landesmuseum Darmstadt, Friedensplatz 1, 64283 Darmstadt, Germany

Franco Andreone, Sezione Zoologia, Museo Regionale di Scienze Naturali, Torino, Italy

Angelica Crottini, Cibio, Centro de Investigação em Biodiversidade e Recursos Genéticos, InBio, Universidade do Porto, Vairão, Portugal

Louis du Preez, School of Environmental Sciences and Development, North-West University, Potchefstroom campus, Private Bag X6001, Potchefstroom 2520, South Africa

Michaela Preick & Michael Hofreiter, Institut für Biochemie und Biologie, Universität Potsdam, Karl-Liebknecht-Str. 24-25, 14476 Potsdam, Germany

Mark D. Scherz, Natural History Museum of Denmark, University of Copenhagen, Universitetsparken 15, 2100, Copenhagen Ø, Denmark

Mark-Oliver Rödel, Museum für Naturkunde – Leibniz Institute for Evolution and Biodiversity Science, Invalidenstraße 43, 10115 Berlin, Germany

Jeffrey W. Streicher, Department of Life Sciences, The Natural History Museum, Cromwell Road, London, UK

Frank Glaw (corresponding author), Zoologische Staatssammlung München (ZSM – SNSB), Münchhausenstr. 21, 81247 München, Germany; e-mail: glaw@snsb.de

Introduction

With currently 16 recognised nominal species (Scherz et al. 2018), the subgenus *Duboimantis* is the most species-rich subgenus in the Madagascar-endemic mantellid genus *Gephyromantis*. In recent years, revisions of several species complexes have revealed new species of *Duboimantis* (e.g., Scherz et al. 2017, 2018), with one notable exception: the species associated with *Gephyromantis luteus* and *G. plicifer*, herein named the *G. plicifer* complex after the historically first named species, have not been revised since Vences & Glaw (2001). These authors followed Blommers-Schlösser & Blanc (1991) who considered these species to be part of the “*Mantidactylus asper* group”, supposedly related to other species that according to more recent phylogenetic knowledge belong to a separate subgenus, *Asperomantis* (Vences et al. 2017).

Currently (Frost 2021, AmphibiaWeb 2021), the *G. plicifer* complex comprises three species (*G. luteus*, *G. plicifer*, *G. sculpturatus*) forming a clade that is sister to all other species of *Duboimantis* (Glaw & Vences 2006, Kaffenberger et al. 2012). However, DNA barcoding data have already indicated the existence of at least two further deep genetic lineages of uncertain taxonomic status, named *Gephyromantis* sp. 20 and sp. 21 by Vieites et al. (2009). Herein we refer to them as *G. sp. Ca20* and *G. sp. Ca21*, according to the scheme introduced by Perl et al. (2014).

The last taxonomic revision of the alpha taxonomy of the *G. plicifer* complex dates back over 20 years, when Vences & Glaw (2001) distinguished three species, still under the genus name *Mantidactylus*: (1) *Gephyromantis luteus* (Methuen & Hewitt, 1913),

a species supposedly occurring at predominantly low-elevations along Madagascar’s east coast, all the way from the Anosy Massif (Chaines Anosyennes) in the South East to the Marojejy Massif in the North East; (2) *Gephyromantis sculpturatus* (Ahl, 1929), a species morphologically very similar to *G. luteus* but distributed at mid-elevations in the northern Central East (Andasibe, Ankeniheny) and southern Central East (Ranomafana); and (3) *Gephyromantis plicifer* (Boulenger, 1882), a species supposedly reaching larger sizes than the previous two species, and known from the southern Central East (Ranomafana) and South East (Anosy Massif). These taxonomic hypotheses, however, suffered from multiple uncertainties and inconsistencies, including: (i) the uncertain type locality of *G. sculpturatus* (the species was described, probably mistakenly, from northwestern Madagascar), (ii) lack of recent collections of topotypical material of *G. luteus* (from near the historical type locality Foholy), (iii) deviant morphology of the lectotype of *G. plicifer*, which is smaller in size than other specimens assigned to this species, (iv) uncertain status of the two candidate species *G. sp. Ca20* and *G. sp. Ca21*, and (v) most importantly, lack of a comprehensive screening of genetic variation across the full distribution area of the complex.

Given that there are doubts concerning the identity of the name-bearing types of all three nomina in the *G. plicifer* complex, and that the high morphological similarity of all lineages in this complex makes a reliable assignment based only on morphological characters impossible, obtaining molecular data from the types is an essential requirement for a thorough taxonomic revision.

In the present study we provide such data based on a “DNA barcode fishing” (Rancilhac et al. 2020, Scherz et al. 2020) strategy to sequence a marker gene fragment from liquid-preserved historical collection material, and complement this information with a comprehensive analysis of mitochondrial and nuclear-encoded DNA sequences from across the distribution range of the complex, as well as extensive bioacoustic comparisons. Our study confirms multiple deep genetic lineages in the complex, one of which we name as a species new to science.

Materials and methods

Sampling and collection acronyms

Samples and voucher specimens studied herein were collected during numerous expeditions to Madagascar between 1996–2016. In the field, frogs were anaesthetised by immersion in MS222 or chlorobutanol solutions and subsequently euthanized by overdose of the same substances. Tissue samples were removed for molecular analysis and stored separately in vials with pure ethanol. Vouchers were fixed in 95 % ethanol, preserved in 70 % ethanol, and deposited at the Zoologische Staatssammlung München (ZSM), Museo Regionale di Scienze Naturali di Torino (MRSN), and the Université d’Antananarivo, Département de Biologie Animale (UADBA). We studied the type material and other relevant specimens of this species complex from the Natural History Museum, London (BMNH), Transvaal Museum Pretoria (TMP), Zoologisches Forschungsmuseum A. Koenig, Bonn (ZFMK), and Museum für Naturkunde Berlin (ZMB). ACZC and ACP refer to field numbers and lab numbers of Angelica Crottini, FAZC to field numbers of Franco Andreone, FGZC, FGMV and ZCMV to field numbers of Frank Glaw and Miguel Vences, JCR to field numbers of Jana C. Riemann, and PSG to field numbers of Sebastian Gehring. Geographical regions in Madagascar (Central East, North East) were named according to Boumans et al. (2007).

Morphological and bioacoustic methods

Morphometric measurements were taken by MV with the accuracy of 0.1 millimeter using a manual caliper and included the following variables: snout-vent length (SVL); maximum head width (HW); head length from tip of snout to posterior edge of snout opening (HL); horizontal tympanum diameter (TD); horizontal eye diameter (ED); distance between anterior edge of eye and nostril (END); distance between nostril and tip of snout (NSD); distance between both nostrils (NND); forelimb length, from limb insertion to tip of longest finger (FORL); hand length, to the tip of the longest finger (HAL); hind limb length, from the cloaca to the tip of the longest toe (HIL); foot length (FOL); foot length including tarsus (FOTL); and tibia length (TIBL). The webbing formula was given according to Blom-

mers-Schlösser (1979) to ensure comparability with previous species descriptions of Malagasy frogs, and the femoral gland terminology according to Glaw et al. (2000).

Vocalizations were recorded in the field using different tape recorders (Tensai RCR-3222, Sony WM-D6C) equipped with external microphones (Sennheiser ME-80, Vivanco EM 238) or with a digital recorder with built-in microphones (Edirol R-09). Recordings were sampled or re-sampled at 22.05 kHz and 32-bit resolution and computer-analysed using the software Cool Edit Pro 2.0. Frequency information was obtained through Fast Fourier Transformation (FFT; width 1024 points) at Hanning window function. Spectrograms were obtained at Blackman window function with 256 bands resolution. In most cases, sensitive filtering was applied to remove background sounds, with filtering exclusively applied to frequencies outside the prevalent bandwidths of calls. Temporal measurements were given as mean \pm standard deviation with range in parentheses. Terminology in call descriptions follows the call-centered scheme of Köhler et al. (2017).

Target-enrichment sequencing of historical types

To obtain DNA sequences from the three name-bearing historical types in the *G. plicifer* complex (*G. luteus*, *G. plicifer*, *G. sculpturatus*) we applied targeted enrichment sequencing (Straube et al. 2021), following a ‘barcode fishing’ strategy that we have previously employed successfully (Rancilhac et al. 2020, Scherz et al. 2020). We specifically aimed at sequencing the same 16S rRNA gene fragment that we used in our molecular dataset 1. This strategy relied on targeted enrichment with 5,962 baits of 70 nucleotides in length, with 5 x tiling density (after filtering based on melting temperature and collapsing 99 % identical baits) designed by Arbor Biosciences from sequences of most Malagasy frog species (including various lineages of the *G. plicifer* complex). Thigh muscle tissue samples were extracted from historical types using DNA-free scissors and stored in 100 % ethanol in 1.5 ml tubes filled in a lab naïve to *Gephyromantis* research. All subsequent wet lab steps were carried out in a dedicated laboratory for ancient DNA analysis at Potsdam University where no other *Gephyromantis* sample had been extracted before. Samples were washed with Qiagen PE Buffer and DNA extracted following the protocol of Rohland et al. (2004) and purified following the protocol of Dabney et al. (2013). Libraries were prepared using a single-stranded DNA (ss-DNA) approach optimized for ancient and archival DNA (Gansauge & Meyer 2013, Gansauge et al. 2017) using custom adapters from Gansauge & Meyer (2013), amplified with custom Illumina indexing primers described in Paijmans et al. (2017), after determining the optimal cycle number using qPCR (Gansauge & Meyer 2013, Basler et al. 2017).

These single-stranded DNA libraries were then captured twice for the aforementioned target sequences using the Arbor Biosciences MyBaits kit, with 14.5 μ L of each indexed library in a 24 h reaction

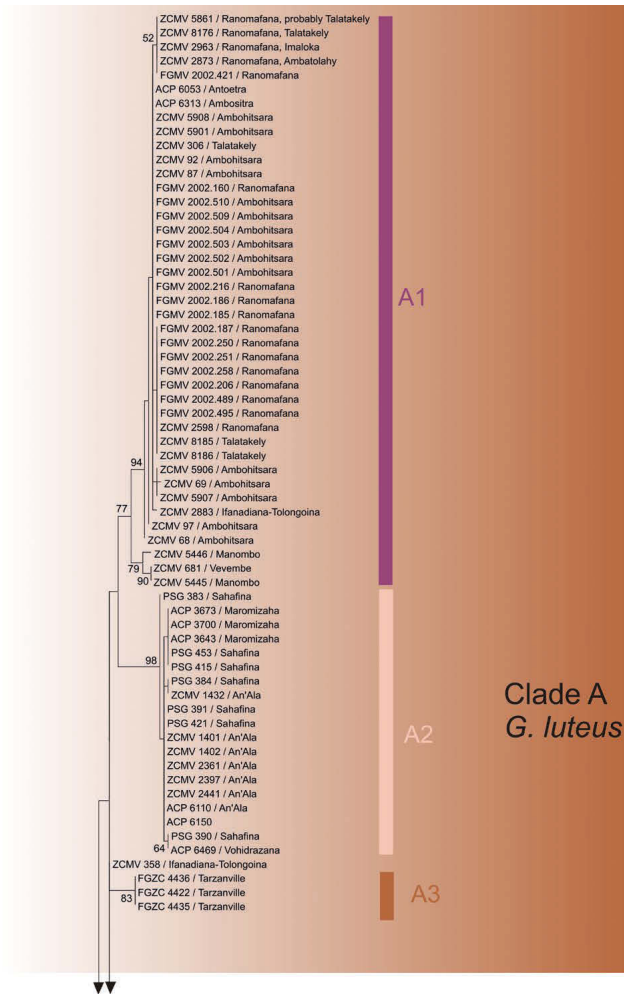


Fig. 1. Maximum Likelihood tree based on DNA sequences of the 3' terminus of the mitochondrial 16S rRNA gene (dataset 1; alignment length 517 nucleotides) of 164 sequences of the *Gephyromantis plicifer* complex, obtained from 161 fresh samples and three name-bearing primary type specimens. Numbers at nodes are bootstrap support values in percent (500 replicates; not shown if < 50 %). Sequences of name-bearing type specimens obtained by target-enriched DNA sequencing are bolded.

at a hybridization temperature of 65 °C, and following the MyBaits target enrichment protocol except reducing the bait volume to 2.75 µL and substituting the missing 2.75 µL in each reaction with nuclease-free water. After hybridization, the libraries were bound to streptavidin-coated magnetic beads, and the reactions washed and eluted according to the MyBaits kit protocol. We then performed amplification PCR in a reaction volume of 60 µL with the following PCR conditions (preceded by the determination of the optimal cycle number, n, using qPCR for each sample): 95 (120), n x [95 (30), 60 (45), 72 (45)], 72 (180). Amplifications were purified using a Min Elute

PCR Purification Kit (Qiagen), with final elution in a total volume of 30 µL of 10 nM Tris-CL, 0.05 % TWEEN-20 solution (pH 8.0). This procedure was performed twice to increase target capture reactions success, as described in Li et al. (2015) and Pajmans et al. (2016). We used a Qubit 2.0 and 2200 TapeStation (Agilent Technologies) assays to determine the final library concentration and length distribution, and sequenced the enriched library on an Illumina Next-Seq 500 sequencing platform using 500/550 High Output v2.5 (75 cycles SE, aimed at 3 million reads per sample) with custom sequencing primers (Pajmans et al. 2017).

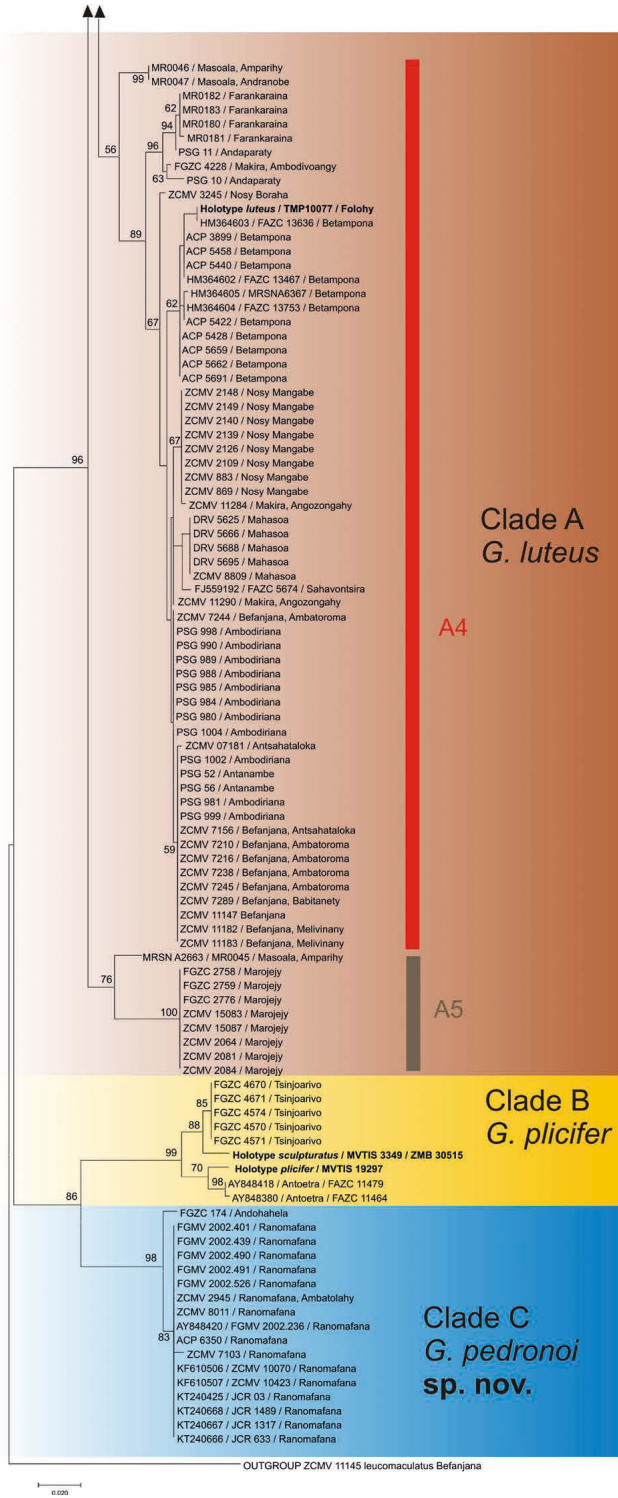


Fig. 1. continued

We used the “Museoscript” custom script (Rancilhac et al. 2020, <https://github.com/rancilhac/Museoscript>) to quality-trim reads, remove adapters, and compare reads via BLAST against a library of selected *Gephyromantis* 16S reference sequences from sequences obtained via classical Sanger sequencing during previous work (*G. “plicifer”*, GenBank accession numbers KF610506 and AY848419; *G. luteus*, MZ019423; *G. malagasius*, AY848353; *G. striatus*, MZ019379; *G. bouleengeri*, AY848379) with a similarity threshold to the references of 90 %, to reduce the data set for further analysis. The selected reads were then submitted in CodonCode Aligner 6.0.2 (CodonCode Corp.) to a majority-based alignment approach to align reads to reference sequences of *G. luteus* and *G. sp. Ca21*. The majority rule approach chosen implies that in cases of conflicting information (multiple nucleotides per site across mapped reads), the nucleotide present in the majority of reads covering this position was chosen. All contigs were visually inspected, and such conflicts found to always correspond to single or very few reads with missing data or probable sequencing errors; no obviously poorly mapping reads were present in the contigs. The consensus sequences obtained were deposited in GenBank (accession numbers OK642424–OK642426). For further analysis, these sequences were then added to the dataset 1 alignment and phylogenetically analysed along with dataset 1, described below.

Molecular datasets

Three molecular datasets were assembled to examine the genetic variation and differentiation within the *G. plicifer* complex:

(1) All 164 available samples were DNA barcoded using a fragment of the 3′ terminus of the mitochondrial 16S rRNA gene, which has previously been used as standard marker for Madagascar’s frogs (Vieites et al. 2009). With the exception of the extraction of the three historical types (see above), the DNA of the other tissue samples was salt-extracted and the 16S fragment amplified using the primer pairs: 16SFrogL1/16SFrogH1 (5′–CATAATCACTTGTCTTTAAA–3′; 5′–GATCCAACATCGAGGTCG–3′), or 16SAr 5′–CGCCTGTTATCAAAAACAT–3′ and 16SBr 5′–CCGGTYTGAAGTCAAGATCAYGT–3′, both modified from Palumbi et al. (1991), and the following PCR protocol: initial denaturation at 94 °C (90 sec), followed by 36–40 cycles of denaturation at 94 °C (45 sec), primer annealing at 50–53 °C (45 sec) and elongation at 72 °C (90 sec), followed by a final extension step at 72 °C (5 min).

(2) To obtain a more reliable estimate of the relationships among the deeper lineages in the complex, the following mitochondrial gene fragments were sequenced for representatives of each major lineage identified based on dataset 1: a fragment roughly corre-

sponding to the the first half (5′) of the 12S rRNA gene, a fragment of the 5′ terminus of the 16S rRNA gene, the DNA barcoding segment of cytochrome c oxidase subunit 1 (*cox1*), and a fragment of cytochrome b (*cytb*). For the latter, amplification and sequencing was only successful in a limited number of lineages. Primers used were 12SAL (5′–AAACTGGGATTAGATACCCCATAT–3′) and 12SBH (5′–GAGGGTGACGGGCGGTGTGT–3′) of Kocher et al. (1989) and Hrbek & Larson (1999) with PCR protocol 94(90), 33x[94(45), 52(45), 72(90)], 72(300); 16SL3 (5′–AGCAAAGAHYWWACCTCGTACTTTTGCAT–3′) and 16SAH (5′–ATGTTTTGTATAAACAGGCG–3′) of Vences et al. (2003) with PCR protocol 94(90), 33x[94(45), 52(45), 72(90)], 72(300); *Cytb-a* (5′–CCATGAGGACAAAATATCATTYTRGG–3′) and *Cytb-c* (5′–CTACTGGTTGCTTCGATTCATGT–3′) of Bossuyt & Milinkovitch (2000) with PCR protocol 94(90), 35x[94(30), 53(45), 72(90)], 72(600); LCO1490 (5′–GGTCAACAAATCATAAAGATATTGG–3′) and HCO2198 (5′–TAAACTTCAGGGTGACCAAAAAATCA–3′) of Folmer et al. (1994) with PCR protocol 94(90), 35x[94(30), 49(45), 72(90)], 72(600).

(3) To confirm that the variation in nuclear-encoded genes was consistent with that of mitochondrial genes, we amplified a fragment of the recombination-activating gene 1 (*Rag-1*) with the newly developed primers *Geph lut-RAG1-F1* ATGGAGAGCCAACCCCTATC and *Geph lut-RAG1-R1* (KCCAGACTCGTTTCCTT-CRC) with PCR protocol 94(120), 35x[94(20), 53(50), 72(180)], 72(600).

All PCR products were purified with Exonuclease I and Shrimp Alkaline Phosphatase digestion. Mitochondrial fragments were sequenced with forward primers only, the nuclear-encoded *Rag-1* fragment was sequenced in both directions and the two strands combined. Sequencing was performed on automated DNA sequencers at LGC Genomics (Berlin). We checked and edited chromatograms with CodonCode Aligner 3.7.1 (Codon Code Corporation, Dedham, MA, USA) and submitted newly determined sequences to GenBank (accession numbers OK559999–OK560007, OK642427–OK642568 and OK556481–OK556579).

Phylogenetic analysis and species delimitation

Sequences were quality-checked and trimmed using CodonCode Aligner, and aligned using the Clustal option implemented in MEGA X (Kumar et al. 2018). The alignment was unambiguous and only required a few, single indels for 12S and 16S, and therefore all sites were used for phylogenetic analysis.

For dataset 1, to avoid overparametrization in the analysis of shallow branches, we ran the analyses with a relatively simple (K2P) substitution model in a Maximum Likelihood (ML) analysis in MEGA X with NNI branch swapping, with 500 nonparametric bootstrap replicates to assess node support. Uncorrected pairwise distances between the 16S sequences of dataset 1 were calculated using the program TaxID2, implemented in iTaxoTools (Vences et al. 2021).

For dataset 2, we undertook a partitioned Bayesian analysis with MrBayes 3.2 (Ronquist et al. 2012), determining the best partition and substitution models with Partitionfinder (Lanfear et al. 2012). The selected partition scheme had six partitions, where the first position of cytochrome b was lumped in one partition with 12S+16S sequences (GTR+I+G model), and each other codon position of cytb and cox1 was placed in an own partition, with the following substitution models: HKY (2nd positions cytb), GTR+G (3rd position cytb, and, separately, 3rd position cox1), SYM+G (1st position cox1), F81+I (2nd position cox1). We ran 5 million generations, sampling every 10,000th tree, and applying a 25 % burn-in after empirical verification of convergence.

Dataset 3, composed of sequences of the nuclear-encoded gene Rag-1, was analysed separately from the mitochondrial genes since our main interest was to assess concordance in the signal held by nuclear-encoded vs. mitochondrial genes. We used a haplotype network visualization to graphically represent the relationship among alleles (haplotypes) of this gene. For this, we first used the presence of overlapping peaks in both forward and reverse strand electropherograms to identify putatively heterozygous sites. We then inferred alleles of the nuclear gene using the PHASE algorithm (Stephens et al. 2001) implemented in DnaSP (Version 5.10.3; Librado & Rozas 2009). The phased sequences were used to reconstruct a ML tree with the JC69 substitution model in MEGAX, which in turn, together with the respective alignment, constituted the input for Haploviewer (written by G. B. Ewing; <http://www.cibiv.at/~greg/haploviewer>), a software that implements the methodological approach of Salzburger et al. (2011).

In this study we followed the general lineage concept (de Queiroz 1998, 2007) in combination with a relaxed biological species criterion, i.e., requiring reproductive isolation indicated by restricted gene flow among lineages (e.g., Speybroeck et al. 2020). Because reproductive barriers generated through time increase genealogical depth and agreement among unlinked loci (Avice & Wollenberg 1997), we used genealogical concordance (Avice & Ball 1990) between mitochondrial and nuclear loci, especially in populations occurring in sympatry or close geographical proximity, as an indicator for restricted gene flow. This was then used to assign species status to a lineage, along with concordance between genetic and morphological evidence (Padiál et al. 2010).

Results

Molecular differentiation

For the sample of the *Mantidactylus sculpturatus* holotype (ZMB 30515), of the total number of 3027450 raw sequence reads, 560916 reads were kept for downstream analysis after filtering, and the consensus sequence was built with 560093 of these reads. Coverage was highly variable, from a minimum of 60 in some stretches to over 190000 in other parts;

overall, more than half of the consensus sequence was reconstructed from a coverage >100000. After filtering, the lectotype of *Rana plicifera* (BMNH 1882.3.16.58) yielded 619745 reads (number of raw reads: 1751967), and the holotype of *Mantidactylus luteus* (TMP 10077) 84282 reads (raw reads: 1491566), which were processed with the same procedure to produce consensus sequences. Coverage for these two consensus sequences, as with *sculpturatus*, was rather variable, but large stretches had very high coverages and were thus very reliably reconstructed.

Together with the samples of the three name-bearing historical types and one outgroup, dataset 1 contained 165 sequences for an alignment length of 517 nucleotides of the 16S gene. The ML tree inferred from this dataset (Fig. 1) revealed three deep clades (supported by bootstrap values of 96–99 %) separated by very high genetic divergences: (A) a clade, which contained all samples assigned to *G. luteus* and *G. sculpturatus* (based on current taxonomy), including the sample from Sahavontsira previously named as *G. sp. Ca20* (Vieites et al. 2009), (B) a clade containing samples assigned to *G. plicifera*, and (C) a clade corresponding to *G. sp. Ca21* (see Vieites et al. 2009), containing samples from Madagascar's southern Central East. Uncorrected pairwise divergences between these three clades ranged between 9.0–14.4 %. See Fig. 2 for geographic distribution of the three clades.

The three historical type specimens were firmly embedded within these main clades (Fig. 1): (i) the holotype of *Mantidactylus luteus* Methuen & Hewitt, 1913 from Folohy was placed in clade A, close to samples from Betampona, which is thought to be geographically close to the historical site Folohy (Blommers-Schlösser & Blanc 1991); (ii) the holotype of *Mantidactylus sculpturatus* Ahl, 1929 was placed in clade B, next to samples from the Tsinjoarivo area; (iii) the lectotype of *Rana plicifera* Boulenger, 1882 was also placed in clade B, close to samples from the Antoetra area.

Within the three main clades, additional deep divergences were detected: in clade A, multiple geographical lineages (here named A1–A5) were detected, of which the one from the north-eastern Marojejy Massif (A5, see next paragraph) was the most divergent, differing by 4.1–7.4 % uncorrected pairwise divergence from all other samples of clade A; within the remaining samples of this clade, divergences were also high, amounting to up to 6.2 %. Within clade C, samples from the Ranomafana area differed from those collected at Andohahela by a maximum of 3.4 %; and within clade B, samples from Antoetra differed from those originating from Tsinjoarivo by up to 1.6 %.

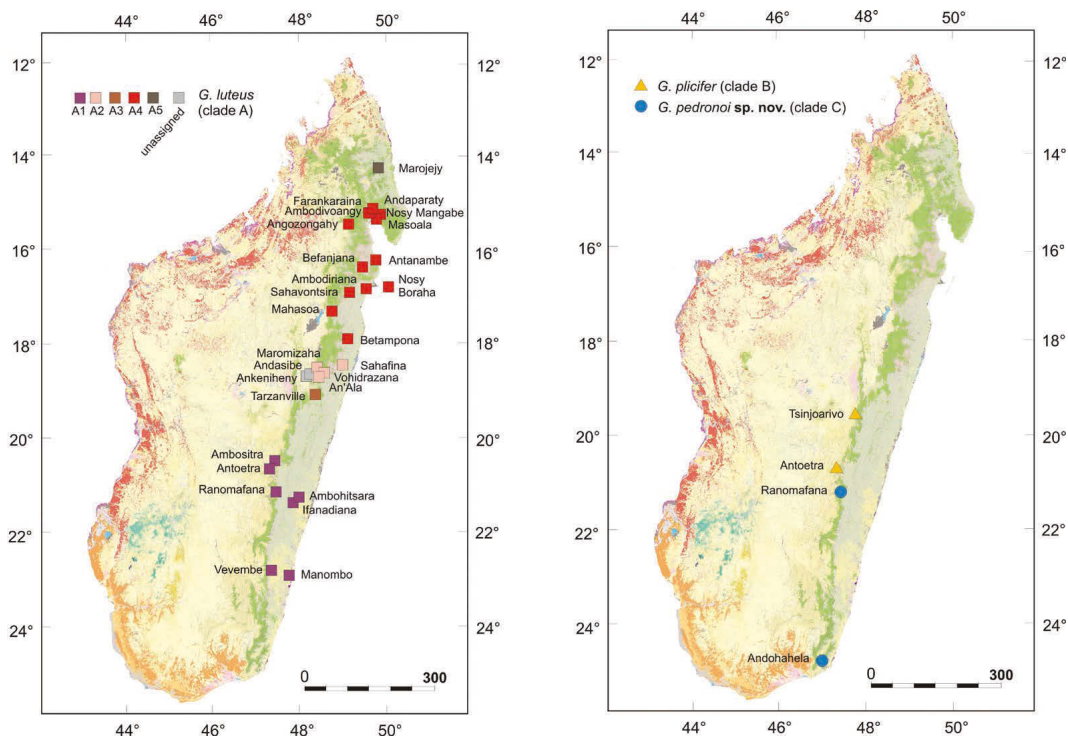


Fig. 2. Maps of Madagascar, showing locality records of the *Gephyromantis plicifer* complex for which samples were identified by DNA barcoding, plus localities Andasibe and Ankeniheny (grey squares) for which call recordings were analysed. The locality Folohy (historical type locality of *G. luteus*) is not shown as it cannot be precisely located, but is likely close to Betampona (see maps in Blommers-Schlösser & Blanc 1991). Note that in Fig. 1, one sample from Masoala (Amparihy) clusters with A5 rather than A4, while a second sample clusters with A4, suggesting this site might be in a contact zone. Colours in map show remaining primary vegetation following the Madagascar Vegetation Mapping Project carried out from 2003–2006 (Moat & Smith 2007); green is humid forest (rainforest), reddish tones are deciduous dry forest, orange is arid spiny forest-thicket, bluish is western sub-humid forest and yellowish is tapia forest.

Within clade A, for convenience, we defined the following main lineages, each restricted to particular geographical regions: A1, occurring in the southern Central East (e.g., Ranomafana, Ifanadiana, Manombo); A2, occurring in the southern part of the northern Central East (e.g., An'Ala, Maromizaha, Vohidrazana); A3, only known from Tarzanville near Anosibe An'Ala; and A4, occurring in the North East (e.g., Nosy Mangabe) and in the northern portion of the northern Central East (e.g., Mahaso, Makira, Betampona). Lineage A4 contained both the holotype of *luteus* from Folohy, and the reference specimen of *G. sp.* Ca20 from Sahavontsira. Finally, lineage A5, occurs at the Marojejy Massif, together with one genetically divergent sample from Masoala.

The partitioned Bayesian phylogenetic analysis based on 2568 bp of four mitochondrial genes for selected samples (Fig. 3) placed clade B as sister

group to clade A+C, with a posterior probability (PP) of 0.93 for A+C. Within clade A, lineages A2, A3 and A5 were represented by single samples. The sample from the north-eastern Marojejy Massif representing subclade A5 was sister to a clade of all other samples (PP=1.0). Subclades A1 and A2+A3 were sister to each other (PP=1.0), and together were sister to subclade A4 (PP=1.0).

The analysis of nuclear-encoded DNA sequences (477 bp) of the Rag-1 gene from 97 specimens (Fig. 4) revealed absence of haplotype sharing between the mitochondrial clades A, B and C. Within samples assigned to clade A by mitochondrial data, the mitochondrial subclade A1 from the southern Central East appeared largely separate from the other clades, with only very limited haplotype sharing with a few individuals from clade A4. In contrast, haplotypes from A2+A3, A4 and A5 were closely connected,

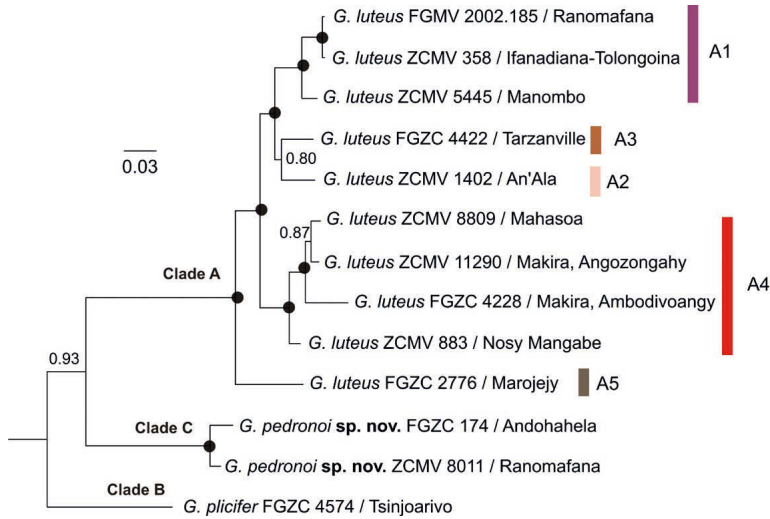


Fig. 3. Majority-rule consensus tree from a partitioned Bayesian phylogenetic analysis based on the concatenation of four mitochondrial genes (dataset 2; 2568 bp) for representative samples of the *Gephyromantis plicifer* complex. Numbers at nodes are Bayesian posterior probabilities, shown as black dots for PP=1.0. The tree was rooted with *G. leucomaculatus* (removed for better graphical representation).

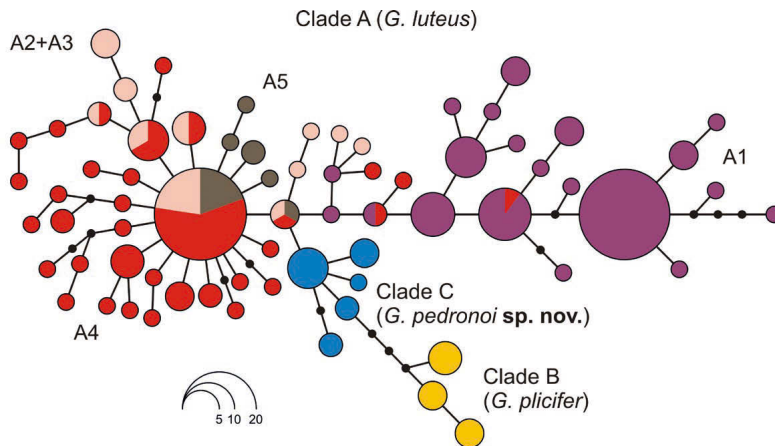


Fig. 4. Haplotype network based on 477 nucleotides of the nuclear-encoded Rag-1 gene from 97 specimens of the *Gephyromantis plicifer* complex (dataset 3). Sequences were phased into haplotypes before analysis; each specimen is therefore represented twice in the network. Size of circles corresponds to number of sequences of the same haplotype. Colours correspond to mitochondrial clades as determined by the analyses of dataset 1 (Fig. 1).

with multiple occurrences of haplotype sharing and without an apparent signal of separation in this nuclear-encoded gene.

Morphological differentiation

We did not undertake a novel study of morphological variation but instead relied on the results of Vences & Glaw (2001) who analysed measurements of 41

specimens of the complex from multiple localities, and found two main characters differentiating lineages: (i) body size is larger in adult specimens corresponding to clade C (>44 mm SVL) compared to that of specimens assigned to clades A and B (<44 mm SVL); and (ii) femoral glands of males are large and distinct in individuals of clades B and C (ratio of femoral gland length FGL to SVL >0.05), and inconspicuous and small in individuals of clade

A (FGL/SVL <0.05 in almost all males measured). The combination of these two characters thus allows the reliable assignment of almost all known male voucher specimens to one of the three clades (as females lack femoral glands, female individuals of clades A and B cannot be reliably distinguished morphologically). No morphological characters are known to differentiate among individuals genetically assigned to different subclades of clade A.

A further potentially diagnostic character is ventral colour in life (Figs 5–7). Two female specimens of clade B photographed at Tsinjoarivo (Fig. 6) show reddish ventral colour on hindlimbs, which seems to be absent in all specimens of clades A and C for which data are available (Figs 5, 7), but more systematic assessment of this character in additional specimens is necessary to assess its diagnostic value and possible intra-specific variation.

Bioacoustic differentiation

Advertisement call recordings were available from populations within the range of all three main clades (A, B and C) and within most of the mitochondrial subclades of clade A. However, in most cases, the recordings could not be reliably attributed to DNA barcoded voucher specimens; therefore, in clade A where no morphological characters are known to

differentiate among the genetic subclades A1–A5, the attribution of calls to these subclades remains tentative. The following paragraphs summarize the differences encountered between the analysed recordings (see Figs 8–13 for spectrograms and oscillograms); detailed call descriptions are found in the section “Calls” of the new species described below, as well as in Appendix I and Table 1.

Calls assignable to individuals of clade A were available from multiple localities probably corresponding to different subclades, but none of them can be reliably assigned to a DNA barcoded voucher specimen: Vevembe (probably subclade A1), Ankeniheny (possibly A2 or maybe A3), Nosy Boraha (probably A4), and Marojejy (probably A5). Furthermore, recordings were available from Andasibe, which geographically would correspond to A2 or maybe A3, but calls were very similar to calls from Vevembe (A1) with respect to call duration, duration of call series and amplitude modulation (pulse structure). The advertisement call of clade A is a single note with a duration varying among subclades (overall range 18–157 ms) that in some populations is pulsatile, repeated in series of 6–26 calls at fast succession (call repetition rate 150–330 calls per minute) with mostly regular inter-call intervals. Individuals probably assignable to subclades A4 and A5 have the highest call repetition

Table 1. Comparative numerical parameters of analysed advertisement calls of *Gephyromantis pedronoi* sp. nov., *G. plicifer* and various populations of *G. luteus*. Values are provided as range followed by mean \pm standard deviation in parentheses.

species/genetic lineage	locality	call duration [ms]	inter-call interval [ms]	repetition rate [calls/minute]	duration of call series [ms]	number of calls per call series	dominant frequency [Hz]	prevalent bandwidth [Hz]
<i>G. pedronoi</i> sp. nov./Clade C	Ranomafana (a)	84–112 (95.7 \pm 9.2)	881–2091 (1272.3 \pm 421.1)	34–51	8294	7	1326–1438 (1395 \pm 35)	1300–3500
<i>G. pedronoi</i> sp. nov./Clade C	Ranomafana (b)	74–100 (89.7 \pm 9.3)	464–2533 (1291.5 \pm 744.5)	26–94	8469	7	1275–1313 (1287 \pm 12)	1100–3300
<i>G. plicifer</i> /Clade B	Antoetra	150–171 (161.0 \pm 11.0)	128–196 (148.1 \pm 22.9)	ca. 190	1776–2834	5–9	2897–3127 (2987 \pm 65)	1100–5000
<i>G. luteus</i> /Subclade A1	Vevembe	85–157 (111.9 \pm 19.7)	195–253 (220.5 \pm 17.0)	ca. 180	5745–5952	18	3079–3660 (3321 \pm 173)	1300–3800
<i>G. luteus</i> /Subclade uncertain	Andasibe	93–147 (116.8 \pm 15.9)	226–295 (272.3 \pm 28.9)	ca. 150	5743	15	3186–3294 (3215 \pm 42)	1300–5400
<i>G. luteus</i> /Subclade uncertain	Ankeniheny	103–140 (114.5 \pm 13.5)	184–238 (208.6 \pm 16.6)	ca. 187	5931–7655	19–26	3057–3402 (3117 \pm 367)	1400–4800
<i>G. luteus</i> /Subclade A4	Nosy Boraha	41–49 (43.3 \pm 2.8)	144–379 (203.6 \pm 63.4)	140–330	1122–2505	6–12	3488–3811 (3615 \pm 136)	1630–1840
<i>G. luteus</i> /Subclade A5	Marojejy	18–35 (25.8 \pm 5.6)	159–191 (175.1 \pm 10.0)	290–300	2067–4086	11–21	3337–3596 (3350 \pm 451)	1400–7600

rate (140–330 calls/minute in A4, 290–300 calls/minute in A5), shortest calls that usually have only a weakly expressed pulsatile structure (call duration 41–49 ms in A4, 18–35 ms in A5). In contrast, calls of subclades A1 and A2/A3 have calls almost doubling in duration (85–157 ms), also repeated at a high rate (approximately 180–190 calls/minute), and exhibiting a more distinct pulsatile structure with some differences among recordings. All calls assignable to individuals of clade A exhibit a pronounced upward frequency modulation.

From clade B, only one recording was available (from Antoetra). The calls cannot be assigned to a precise voucher specimen, but were recorded from a series comprising the DNA barcoded male specimens MRSN A2243 (FAZC 11464; SVL=42.4 mm) and MRSN A2244 (FAZC 11479; SVL=37.1 mm), although we cannot fully exclude that the calls were emitted from other, not collected individuals. They consist of a single pulsatile note of around 160 ms duration that was emitted in short series at rapid succession (call repetition rate within a series is about 190 calls per minute), and that show a considerable upward frequency modulation where the dominant frequency starts at around 2400 Hz and increases up to around 3100 Hz. The long call duration and upward frequency modulation of these calls are reminiscent of the calls of subclades A1 and A2/A3 in clade A, but call duration is above the upper limit observed in clade A, and the frequency modulation is more distinct.

Advertisement calls of specimens that could be unambiguously assigned to clade C by geographical occurrence and morphology (body size, distinctness of glands; see next section) were available from Ranomafana National Park, recorded on two different occasions (in 1996 and 2003). As already described by Vences & Glaw (2001), these calls consist of a short single pulsatile note of about 100 ms duration that is usually emitted in short series and irregular intervals, with a call repetition rate of only 26–94 per minute. Calls exhibit distinct downwards frequency modulation with the parallel frequency bands dropping towards the end of calls. Among the available recordings of the *G. plicifer* complex, the low repetition rate, irregular repetition of calls and downward frequency modulation, is uniquely observed in clade C.

Taxonomic conclusion

The full concordance among various lines of evidence, i.e. reciprocal monophyly in mitochondrial phylogeny, high mitochondrial divergences, lack of haplotype sharing in a nuclear-encoded gene, as well as bioacoustic and morphological differences, leave

no doubt that clades A, B and C are to be regarded as distinct biological species. This conclusion, along with the DNA sequences obtained by DNA barcode fishing from the historical types, suggest a taxonomic scenario for the *G. plicifer* complex that differs substantially from current taxonomy: (1) Clade A contains the holotype of *Mantidactylus luteus* Methuen & Hewitt, 1913, as well as the reference specimen of *G. sp. Ca20*; both these samples are included in subclade A4. The name *Gephyromantis luteus* thus is to be applied to clade A, and more specifically to subclade A4. The status of the various subclades of *G. luteus* (A1–A5) remains uncertain due to a lack of clear and concordant differentiation in the analysed dataset and will be elaborated in the “Discussion”. (2) Clade B, corresponding to *G. sp. Ca21*, includes the name-bearing type of *Rana plicifera* Boulenger, 1882, and also agrees with it morphologically, leaving no doubt that this clade should be named *Gephyromantis plicifer*. (3) The holotype of *Mantidactylus sculpturatus* Ahl, 1929 is also included in clade B, and thus is to be regarded as junior synonym of *G. plicifer*. (4) Consequently, no scientific name is available for populations belonging to clade C, and these are therefore formally named as a new species in the following.

Gephyromantis pedronoi sp. nov.

Figs 7, 14

Identity. This species has previously been assigned to *Gephyromantis plicifer* in various publications (e.g., Vences & Glaw 2001, Vences et al. 2006, Glaw & Vences 2007), based on the analysis of Vences & Glaw (2001) who relied on morphological similarities with the lectotype of *Rana plicifera* Boulenger, 1882 (distinct and large femoral glands of type 2), but also already remarked the smaller body size of the *plicifer* lectotype. It corresponds to the genetic clade C and is here recognised as distinct at the species level from *G. plicifer* (clade B).

Holotype. ZSM 1798/2008, field number ZCMV 7103, adult male from a site called Mariavaratra in Ranomafana National Park, southeastern Madagascar, collected on 22 January 2008 by P. Bora. Geographical coordinates of the precise collecting site are not available, but Mariavaratra is located approximately at 21.261°S, 47.419°E.

Paratypes. ZSM 98/2004 (FGZC 174), probably a sub-adult female, collected at Andohahela, between Isaka und Eminiminy (“Camp 2”), at geographical coordinates 24.73833°S, 46.84028°E, ca. 600 m a.s.l., between 01–04 February 2004 by F. Glaw, M. Puente, M. Thomas, and R. D. Randrianiaina. ZFMK 62305–62306, two adult males, collected by F. Glaw, D. Rakotomalala and F. Ranaivojoana on 02 March 1996 in Ranomafana National Park.



Fig. 5. Specimens of *Gephyromantis luteus* in life. **a-b.** Adult male from Ranomafana (clade A1) in dorsolateral and ventral view, photographed in 2003. **c-d.** Adult male from Andasibe (probably clade A2), in dorsolateral and ventral view, photographed 1992. **e.** Calling male from Nosy Mangabe (clade A4). **f-g.** Adult male from Nosy Mangabe (clade A4), in dorsolateral and ventral view, photographed 2005. **h-j.** Adult male from Nosy Boraha (clade A4), in dorsolateral, dorsal and ventral view, photographed 1991. The specimen in panels (f, g) probably corresponds to ZSM 5085/2005 (ZCMV 883) while the other individuals cannot be reliably assigned to preserved voucher specimens.



Fig. 6. Specimens of *Gephyromantis plicifer* (clade B) in life. a. Adult male from Antoetra (MRSN A2243); b–c. dorsolateral and ventral views of a female from Tsinjoarivo (ZSM 317/2010 / FGZC 4570); d–e. dorsolateral and ventral views of a female from Tsinjoarivo (UADBA / FGZC 4571).

Additional material. MNHN 1972.1404 (Ambana-Soavala, Chaines Anosyennes); MNHN 1972.1405, 1972.1407–1408, 1972.1410, 1972.1412–1414, 1972.1419–1422, 1972.1424–1425, 1972.1427, 1972.1429, 1972.1431 (Camp V, Chaines Anosyennes); MNHN 1972.1436–1437 (Camp IV, Chaines Anosyennes). All these specimens were collected in 1972 by C. P. Blanc in the Anosy Mountain Chain during a 1971–1972 scientific expedition to this massif and based on morphological characters (Vences & Glaw 2001) most likely belong to this species; however, since no genetic or bioacoustic data are available for these specimens, we assign them only tentatively and do not include them in the paratype series.

Etymology. The name is a patronym dedicated to Miguel Pedrono in recognition of his substantial contributions to our understanding of the biology of Madagascar's tortoises, in particular the Angonoka, *Astrochelys yniphora*, and his immense efforts in tortoise conservation (e.g. Pedrono 2008, Pedrono & Clausen 2018).

Diagnosis. A species of *Gephyromantis* assigned to the *G. luteus* complex in the subgenus *Duboisimantis* on the basis of presence of intercalary elements between ultimate and penultimate phalanges of fingers and toes present (assessed by external examination), absence of nuptial pads, a single patch of well-delimited femoral glands of type 2 in males (no rudiments in females), paired blackish subgular

vocal sacs in males, fairly smooth skin, moderately large body size, outer metatarsalia separated by webbing, presence of inner and outer dorsolateral ridges, and molecular phylogenetic affinities. Within the *G. luteus* complex, the species can be identified by a unique combination of the following characters: moderately large body size (adult males >43 mm and often up to 44–46 mm, vs. up to 43 mm but often <40 mm in *G. luteus* and *G. plicifer*), distinct and relatively large femoral glands in males (vs. small, often indistinct to unrecognisable externally in *G. luteus*), and emission of advertisement calls in irregular series at low call repetition rate of <100 calls per minute (vs. fast, regular series of at least 140 calls per minute in *G. luteus* and *G. plicifer*), and distinct downward frequency modulation (vs. upward frequency modulation in *G. luteus* and *G. plicifer*).

Description of holotype

Specimen in excellent state of preservation, with a small ventral incision in the right thigh for tissue collection, and skin surrounding right femoral gland partly detached for gland examination. Snout-vent length 46.5 mm. For other measurements see Table 2. Body slender but less so than many other individuals in this species complex; head as long a wide, as wide as the body; snout rounded in dorsal

Table 2. Morphometric measurements (in mm) of holotype (ZSM 1798/2008) and three paratypes of *Gephyromantis pedronoi* sp. nov. Abbreviations of measurements, see Materials and methods. M, male; F, female; NM, not measured; NA, not applicable.

	Holotype		Paratypes	
Catalogue number	ZSM 1798/2008	ZSM 98/2004	ZFMK 62305	ZFMK 62306
Field number	ZCMV 7103	FGZC 174	NA	NA
Locality	Mariavaratra, Andohahela	Ranomafana	Ranomafana	Ranomafana
Sex	M	F	M	M
SVL	46.5	41.3	44.4	44.2
HW	18.0	15.2	17.0	16.6
HL	18.0	16.6	18.0	18.0
HTDt	3.0	2.9	2.8	2.7
ED	5.7	6.5	5.4	5.5
END	4.5	4.9	4.6	4.4
NSD	3.0	2.7	2.8	2.7
NND	4.6	4.5	4.5	4.3
FORL	28.2	27.1	27.5	29.1
HAL	13.6	13.0	13.6	13.7
HIL	81.7	86.2	87.0	86.3
FOTL	37.0	37.1	39.6	38.1
FOL	25.0	24.8	26.5	24.1
TIBL	27.4	28.7	NM	NM
FGL	9.0	NA	8.4	8.3
FGW	4.2	NA	2.8	2.9

and lateral view; nostrils directed laterally, slightly protuberant, much nearer to tip of snout than to eye; canthus rostralis distinct, straight; loreal region concave; tympanum not very distinct but clearly visible, ovoid, its horizontal diameter 67 % of eye diameter; supratympanic fold distinct, relatively straight; tongue ovoid, distinctly bifid posteriorly; vomerine teeth distinct, in two small aggregations, positioned posteromedially to choanae; choanae rounded; maxillary teeth present. Dark dermal fold (the inflatable parts of the vocal sacs) running along each lower jaw from commissure of mouth to middle of lower jaw. Arms slender, subarticular tubercles single; outer metacarpal tubercle very poorly developed and inner metacarpal tubercle relatively well developed; fingers without webbing; relative length of fingers $1 < 2 < 4 < 3$, second finger distinctly shorter than fourth; finger discs distinctly enlarged, nuptial pads absent. Hindlimbs slender; tibiotarsal articulation reaching very slightly beyond snout tip when hindlimb is adpressed along body; lateral metatarsals separated by webbing; inner metatarsal tubercle distinct, outer metatarsal tubercle not recognisable; webbing formula of foot 1 (1), 2i (1), 2e (0.25), 3i (1.75), 3e (0.25), 4i (2), 4e (2), 5 (0); relative toe length $1 < 2 < 3 < 5 < 4$; fifth toe slightly but distinctly longer than third toe; toe discs distinctly enlarged. Skin dorsally rather smooth, with some granules laterally and a fine network of faint ridges on the posterior dorsum. Inner and outer dorsolateral ridge (as defined in Vences & Glaw 2001) distinct. Small but clearly recognisable supraocular tubercles. Ventral skin smooth on throat, chest and limbs, granular on posterior portion of abdomen. Femoral glands of type 2 well delimited externally, consisting of 54 separate granules on the left side.

Dorsal colour after 13 years in preservative, greyish brown, with black colour lining externally the inner dorsolateral ridges, and a small stretch at the start of the outer dorsolateral ridges. A few scattered granules above the forelimb insertion also with some dark brown and light colour. A cream band runs dorsally between the eyes, and a distinct cream patch surrounded by dark brown is present on the upper lip and loreal region. Forelimbs with about 3–4 brown crossbands, hindlimbs with ca. 6 brown crossbands on thigh and 6 brown crossbands on shank. Ventral side uniformly whitish except blackish vocal sacs. Coloration in life not known.

Variation. The diagnostic characters (body size, distinctness of femoral glands) are constant in all examined specimens, including the additional material from the Anosy Massif examined by Vences & Glaw (2001). Including information from this mate-

rial (which has not been genetically identified), SVL ranges between 43.6–48.3 in males, and 44.6–49.8 in females. A further female (ZSM 98/2004, FGZC 174) from Andohahela is smaller (SVL 41.3 mm; Table 2) but might be subadult. For variation in colour pattern, see Fig. 7. In one paratype from Ranomafana (ZFMK 62306), a femoral gland was composed of 47 granules of 0.5–0.7 mm in diameter and in one specimen from the Chaines Anosyennes, a gland was composed of 55 granules of 0.4–0.8 mm in diameter (Vences & Glaw 2001), demonstrating that the number of femoral gland granules can vary between individuals to a certain degree.

Vocalization. The advertisement call recorded on 23 January 2003, 20:15 h, at Ranomafana National Park (air temperature 21.5 °C; Vences et al. 2006: CD2, track 16, cut 1) consists of a short single pulsatile note, usually emitted in series at irregular intervals and slow succession (Fig. 13). Amplitude modulation is recognisable within calls, with call energy being greatest at the beginning of the call and constantly decreasing towards its end. No clear pulse structure is evident in the oscillograms, but the pulsatile nature of calls is evident to the human ear as well as illustrated by numerous parallel frequency bands reflecting high pulse rate (see Köhler et al. 2017). Calls exhibit distinct frequency modulation, namely a downward frequency sweep with the parallel frequency bands dropping towards the end of calls. Numerical call parameters of 7 analysed calls are as follows (range followed by mean \pm standard deviation in parentheses): call duration (= note duration) 84–112 ms (95.7 \pm 9.2 ms); inter-call interval 881–2091 ms (1272.3 \pm 421.1 ms); call repetition rate within call series approximately 34–51 calls/minute; duration of call series 8294 ms ($n = 1$); number of calls per call series 7 ($n = 1$); dominant frequency 1326–1438 Hz (1395 \pm 35 Hz); prevalent bandwidth 1300–3500 Hz, with call energy present up to 8800 Hz.

Additional advertisement calls recorded on 2 March 1996, 18:15 h at 23.5 °C air temperature, also at Ranomafana National Park (Vences et al. 2006: CD2, track 16, cut 2) agree with the calls described above in all general characteristics, including the distinct downward frequency sweep. Numerical parameters of 7 analysed calls are as follows (range followed by mean \pm standard deviation in parentheses): call duration (= note duration) 74–100 ms (89.7 \pm 9.3 ms); inter-call interval 464–2533 ms (1291.5 \pm 744.5 ms); call repetition rate within call series approximately 26–94 calls/minute, with repetition rate increasing towards the end of the series; duration of call series 8469 ms ($n = 1$); number of calls per call series 7 ($n = 1$); dominant frequency 1275–1313 Hz (1287 \pm 12 Hz);



Fig. 7. Three adult males of *Gephyromantis pedronoi* sp. nov. (clade C) from Ranomafana in life, in dorsolateral and ventral views. **a-d.** photographed in 1996; **e-f.** photographed in 2003. The individuals cannot be reliably assigned to preserved voucher specimens, but a-d might correspond to ZFMK 62305–62306.

prevalent bandwidth 1100–3300 Hz.

For detailed comparative advertisement call descriptions of *G. plicifer* and *G. luteus*, see Appendix I and Table 1.

Distribution. The species is reliably known from DNA barcoded specimens from Ranomafana National Park at elevations of about 950 m a.s.l., and Andohahela National Park, from a site between Isaka and Eminiminy at around 600 m a.s.l. Additional specimens probably belonging to this species from the Anosy Chain (Ambana-Soavala, Camp IV, Camp

V) reported above under additional material would originate from a rather wide elevational range, based on the elevational information of campsites reported by Rakotoarison et al. (2017b), i. e., from almost sea level (Ambana) over 550 m (Camp 4) to 1050 m a.s.l. (Camp V).

Natural history and conservation. Very little is known on the natural history of this species. Vences & Glaw (2001) reported that advertisement calls in Ranomafana were heard during dusk from the vegetation in rainforest, emitted from males that were

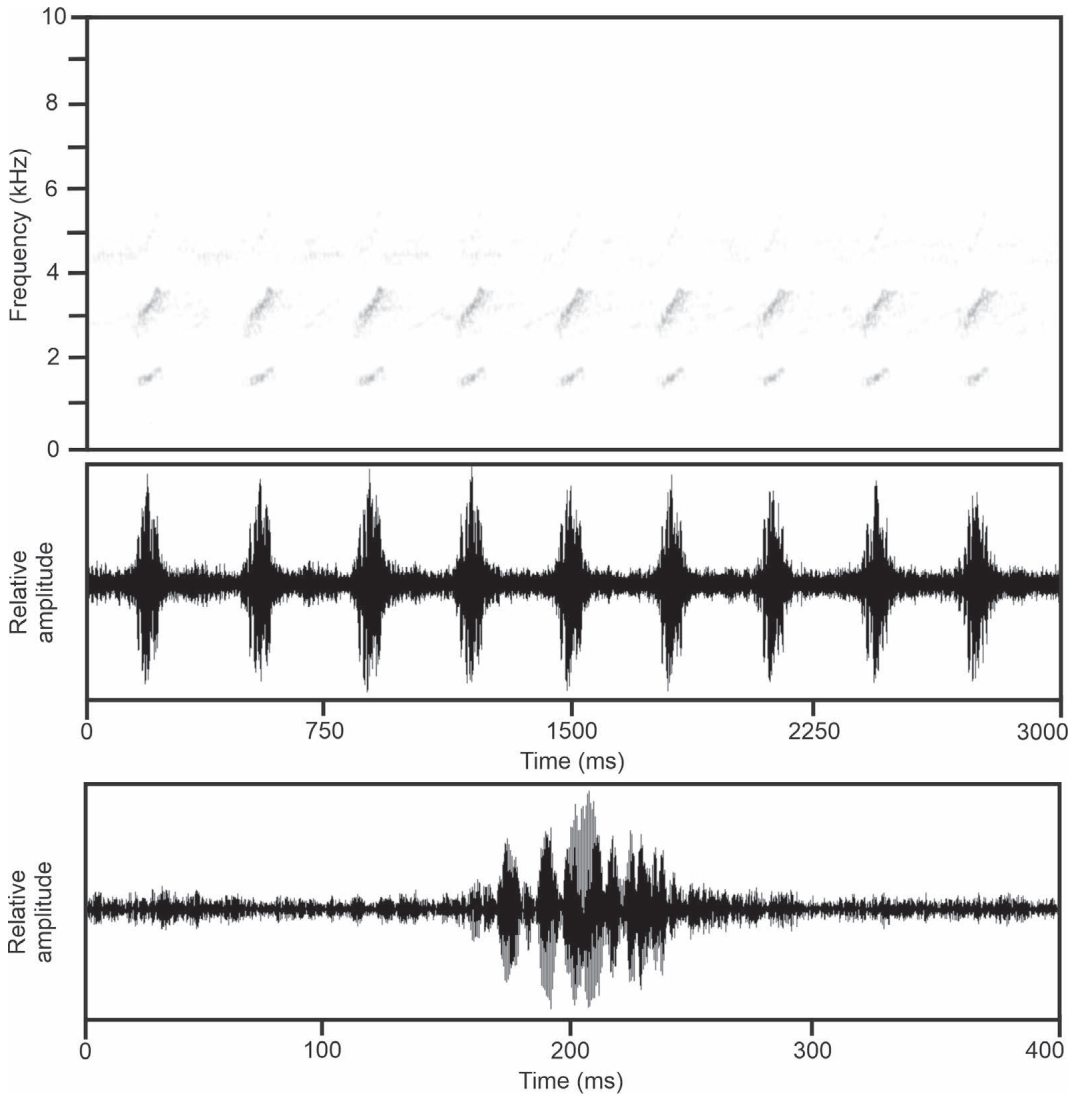


Fig. 8. Audiospectrogram and corresponding oscillogram of a series of advertisement calls of *Gephyromantis luteus* (subclade A1) recorded on 9 February 2004 at Vevembe. Below an oscillogram showing a 400 ms section of the call series above and depicting a single advertisement call; recording was band-pass filtered at 500–7500 Hz.

sitting ca. 50 cm above the ground in the vegetation, far from water bodies. Strauß et al. (2013) reported two tadpoles from Ranomafana identified by DNA barcoding as *G. pedronoi* (ZCMV 10070 and ZCMV 10423; GenBank accessions KF610506–KF610507; and deposited as *G. plicifer*) that conformed to the non-feeding type typically observed in the subgenus *Duboisimantis*, including *G. luteus* (reported as *G. sculpturatus*, see Randrianiaina et al. 2011).

IUCN Red List status: *Gephyromantis pedronoi* is known from at least two protected areas (Ranomafana National Park, Andohahela National Park), and probably occurs in more of the protected areas between these extremes, e.g. Befotaka-Midongy du Sud National Park. *Boophis andohahela* has a similar distribution, occurring in Andohahela, Ranomafana, and Ambatolahy (IUCN SSC Amphibian Specialist Group 2016), and is assessed as Vulnerable under criteria B1ab(iii) of the IUCN Red List (IUCN 2012) due to its distribution <20 000 km² (criterion B1),

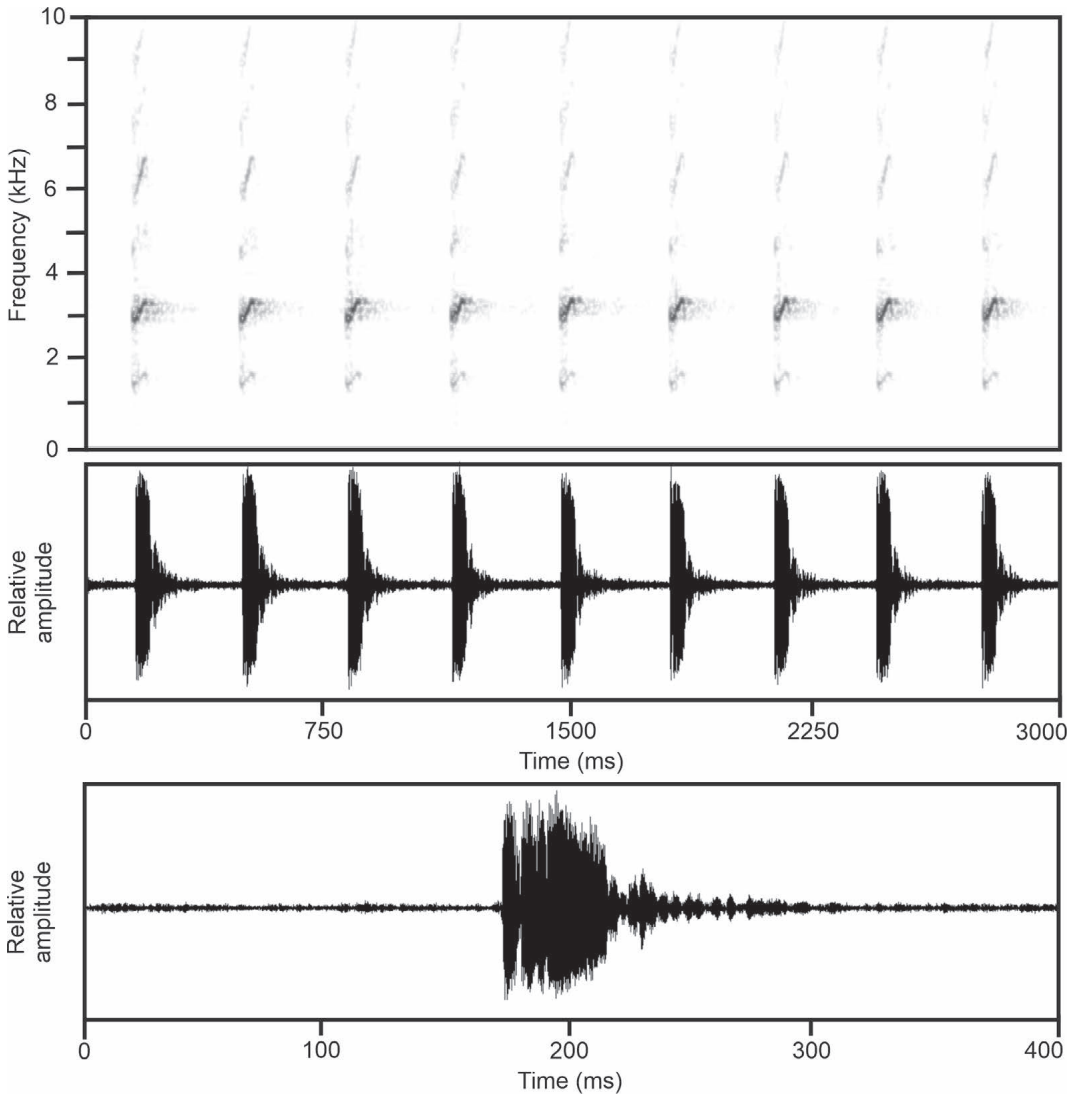


Fig. 9. Audiospectrogram and corresponding oscillogram of a series of advertisement calls of *Gephyromantis luteus* (subclade A2/A3) recorded on 20 February 1994 at Ankeniheny. Below an oscillogram showing a 400 ms section of the call series above and depicting a single advertisement call. Recording was high-pass filtered at 500 Hz.

knowledge from fewer than ten threat-defined locations (subcriterion a), and on-going decline in extent and quality of habitat (subcriterion b(iii)). If *G. pedronoi* is indeed found as low as sea level in suitable habitat, its extent of occurrence may far exceed 20 000 km², but as this remains uncertain, we tentatively recommend it be assessed as Vulnerable B1ab(iii), in keeping with *B. andohahela*.

Discussion

This study provides a preliminary taxonomic revision of a group of widespread but poorly known frogs from Madagascar. Along with other recent work (Rancilhac et al. 2020, Scherz et al. 2020) it demonstrates the power of target enrichment approaches to obtain molecular data from liquid-preserved type material and thereby reliably assign types to lineages identified and delimited based on more recent collections. In the case of the *G. plicifer* complex, this was

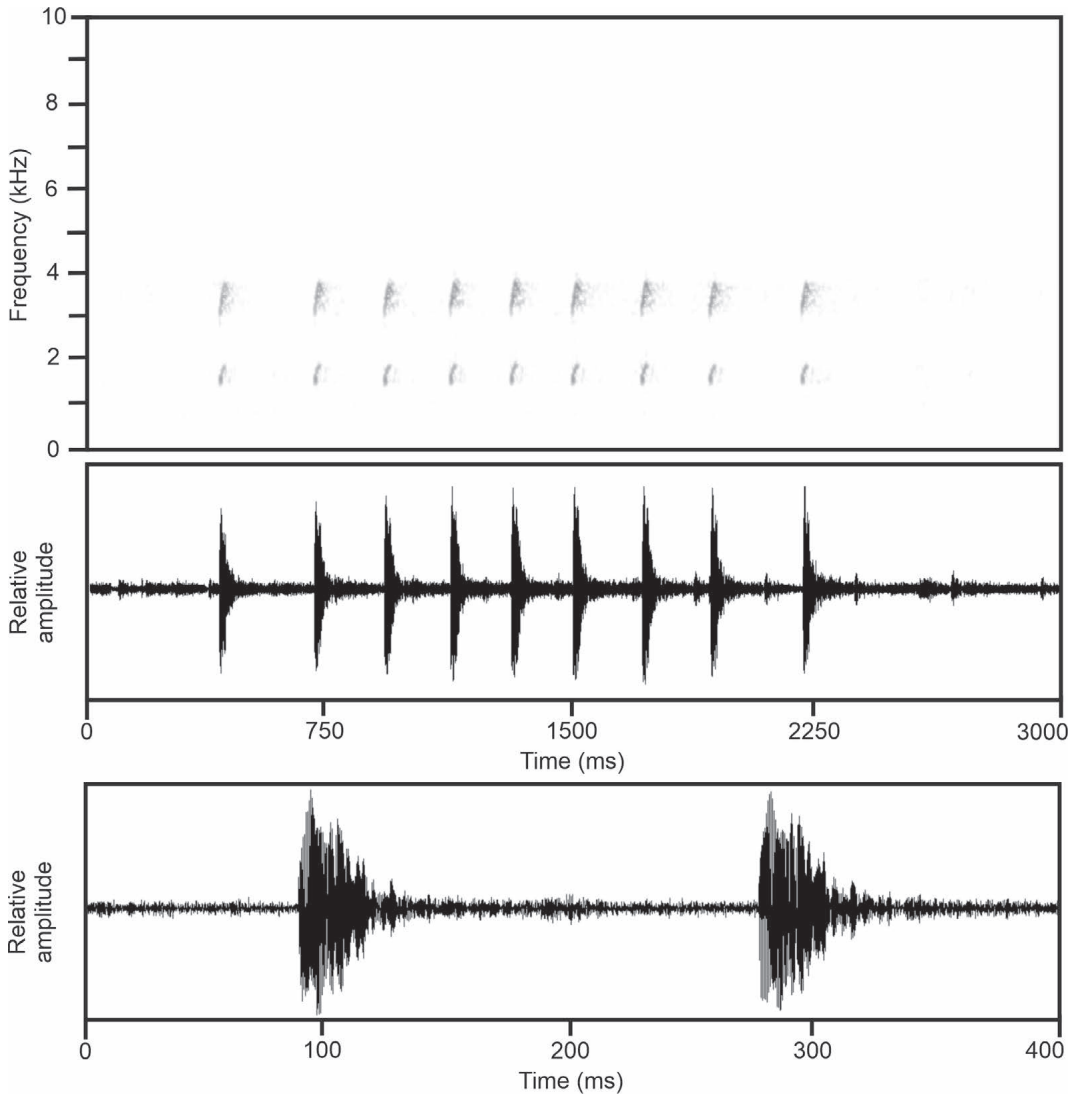


Fig. 10. Audiospectrogram and corresponding oscillogram of a series of advertisement calls of *Gephyromantis luteus* (subclade A4) recorded in February 1991 at Nosy Boraha. Below an oscillogram showing a 400 ms section of the call series above and depicting two advertisement calls. Recording was band-pass filtered at 650–7500 Hz:

particularly important for the type of *Mantidactylus sculpturatus* Ahl, 1929 for which it has been long suspected that the type locality “Nordwest Madagascar” is in error, and geographical arguments could thus not be used reliably to assign it to any lineage. Our barcode fishing strategy also allowed us to resolve the conundrum surrounding the lectotype of *Rana plicifera* Boulenger, 1882, which is similar in distinct femoral glands, but differs by its small body size from frogs occurring in Ranomafana, Anosy Massif and Andohahela (Vences & Glaw 2001), which we

here demonstrate to correspond to a new species, *G. pedronoi*.

While DNA barcode fishing holds a high potential to identify type material, it cannot provide taxonomic resolution where species delimitation itself is convoluted. Here, despite analysis of a rather large number of samples from numerous localities, no taxonomic resolution could be achieved for the mitochondrial subclades of clade A. We here conservatively considered all individuals of subclades A1–A5 as belonging to one species, *G. luteus*; how-

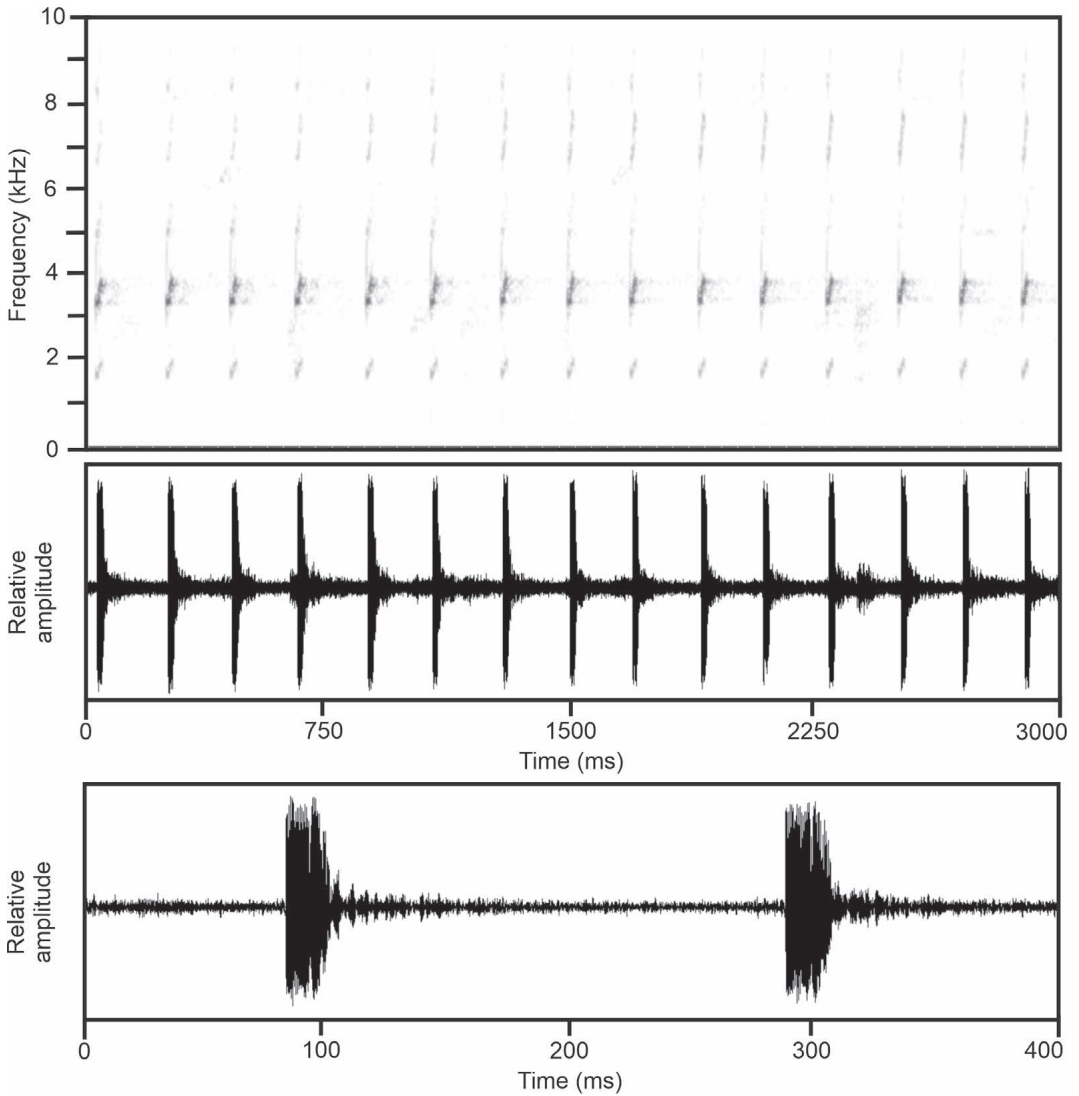


Fig. 11. Audiospectrogram and corresponding oscillogram of a series of advertisement calls of *Gephyromantis luteus* (subclade A5) recorded on 27 March 1994 at Marojejy. Below an oscillogram showing a 400 ms section of the call series above and depicting two advertisement calls. Recording was band-pass filtered at 500–9500 Hz.

ever, the differences between these subclades are consistently larger (pairwise distances always $>4\%$ and up to $>7\%$) than the 3% threshold used by Vieites et al. (2009) to define candidate species among Madagascar's frogs. Furthermore, we encountered bioacoustic differences (already noted by Vences & Glaw 2001) and near-absent Rag-1 haplotype sharing between some of these subclades, suggesting possible species limits separating some of them. However, the available data were too patchy and inconsistent for conclusively drawing a new taxonomic hypothesis

for these frogs.

On the one hand, the mitochondrial data suggested the northernmost population from Marojejy representing the most divergent subclade (A5), but its calls were generally rather similar to those of subclade A4 (even if shorter in duration and repeated more rapidly at equivalent temperatures), and the nuclear-encoded Rag-1 sequences did not provide any evidence for a separation of A5 from A2–A4. On the other hand, the Rag-1 sequences revealed a low extent of haplotype sharing between subclade

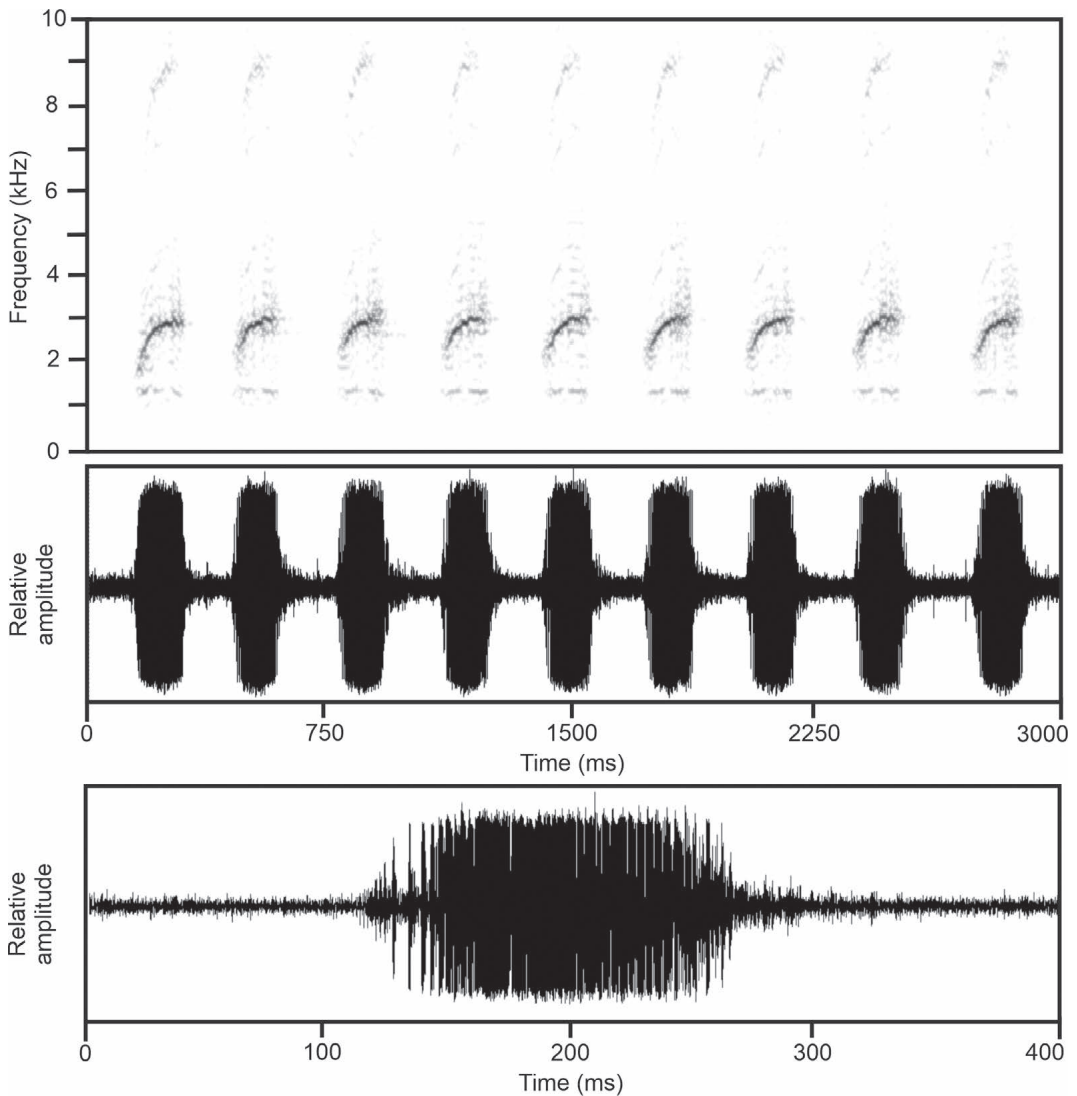


Fig. 12. Audiospectrogram and corresponding oscillogram of a series of advertisement calls of *Gephyromantis plicifer* (clade B) recorded on 30 January 2003 at Antoetra. Below an oscillogram showing a 400 ms section of the call series above and depicting a single advertisement call. Recording was band-pass filtered at 500–10000 Hz.

A1 vs. A2–A5 and the calls of A1 differ in some features to those here provisionally assigned to A2–A5. However, these findings are challenged by the fact that several call recordings cannot be reliably assigned to genetic subclades (especially those from Andasibe and Ankeniheny as no individuals were DNA barcoded from these sites). Geographically, Andasibe is very close to Maromizaha and An’Ala where subclade A2 was found, and it is therefore likely that this subclade also occurs at Andasibe. Interestingly, from their general structure, the calls

recorded at Andasibe appear to be more similar to those from Vevembe (subclade A1). On the other hand, Ankeniheny is close to Moramanga, still close to Andasibe/Maromizaha/An’Ala, but also not excessively far from Tarzanville where subclade A3 was found; individuals from Ankeniheny thus may belong to A3 (given that their calls are somewhat different from those recorded at Andasibe) but could also belong to A2 (the calls representing variation within this subclade).

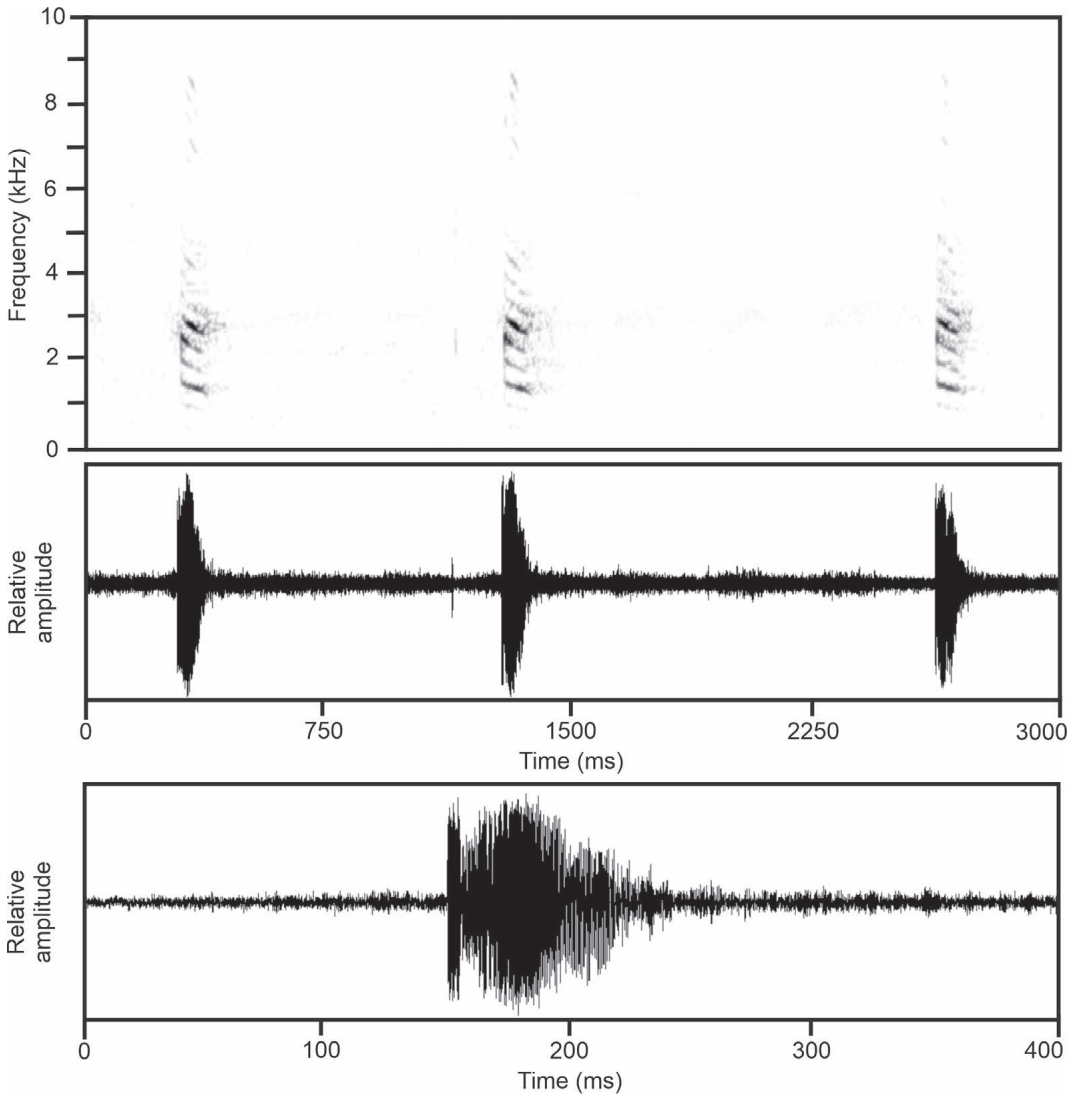


Fig. 13. Audiospectrogram and corresponding oscillogram of advertisement calls of *Gephyromantis pedronoi* sp. nov. (clade C) recorded on 23 January 2003, 20:15 h, at Ranomafana National Park (air temperature 21.5 °C). Below an oscillogram showing a 400 ms section of the call series above and depicting a single advertisement call. Recording was band-pass filtered at 500–9000 Hz.

Our examination of voucher specimens did not reveal any obvious morphological differences between the subclades A1–A5. Vences & Glaw (2001) mention possible variation in the size of femoral gland granules, which however require confirmation from study of a larger number of unequivocally identified individuals, and the exclusion of seasonal influences on this character.

In summary, a rather complex picture is revealed by the data at hand. Without call recordings from

genotyped voucher specimens, any further conclusion with respect to the taxonomic status of the *G. luteus* subclades remains speculative.

Vences & Glaw (2001) separated what we name clade A into two species (at the time still in the genus *Mantidactylus*): *G. luteus*, with short and largely unpulsed calls occurring predominantly at low coastal elevations; and *G. sculpturatus* with longer and more pulsed calls occurring at mid-elevations. The genetic data presented here draw a more complex bioge-

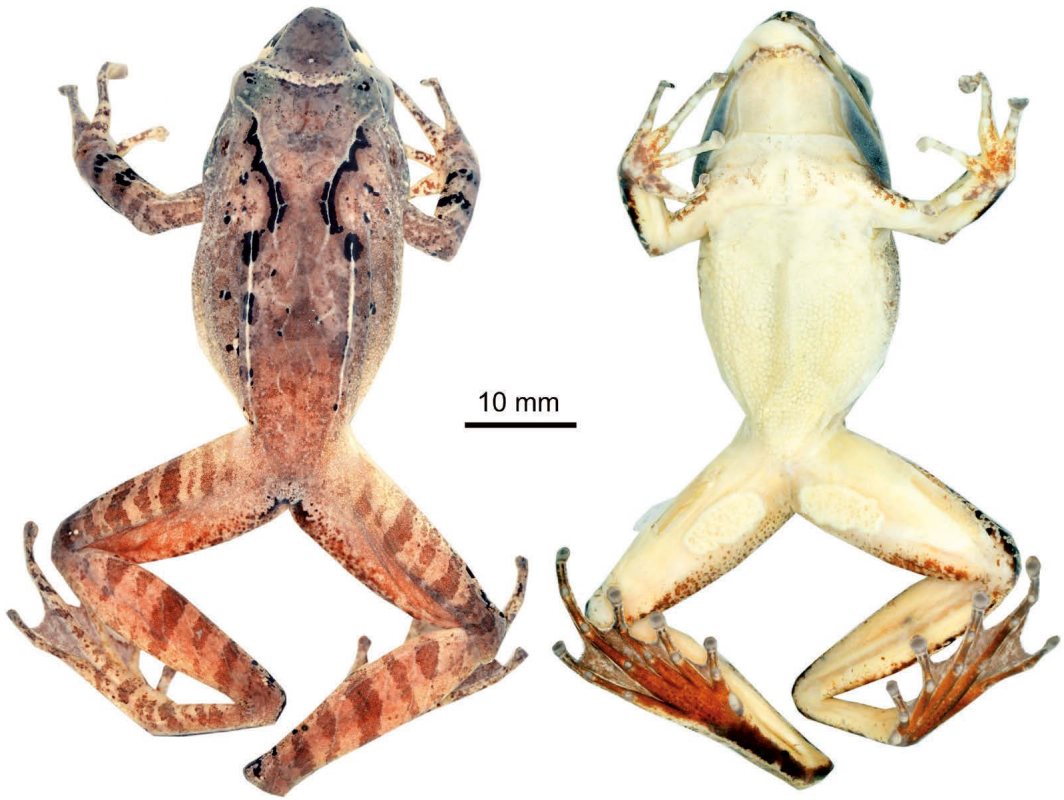


Fig. 14. Preserved male holotype (ZSM 1798/2008, field number ZCMV 7103) of *Gephyromantis pedronoi* sp. nov. from Ranomafana National Park.

graphic picture. For instance, clade A1 (with long and distinctly pulsatile calls) occurs both at the coastal locality Manombo just a few metres above sea level, and at Talatakely in Ranomafana National Park at about 950 m a.s.l. Clade A2 also occupies a rather wide elevational range, from Sahafina (about 60 m a.s.l.) to An'Ala and Maromizaha (>800 m a.s.l.), and clade A4 ranges from Nosy Mangabe around sea level to Angozongahy on the western slope of the Makira Reserve, at around 1000 m a.s.l. However, it seems clear overall that *G. luteus* (clade A) and *G. pedronoi* (clade C) are more common at relatively low elevations <800 m a.s.l., while *G. plicifer* (clade B) occurs at higher elevations (around 1300 m a.s.l. at Tsinjoarivo, and around 1400 m a.s.l. at Antoetra in Farihimazava; Andreone et al. 2007). It is also remarkable that the species of the *G. plicifer* complex have the highest diversity in central eastern Madagascar and are almost entirely absent from far northern Madagascar, where several other groups of reptiles and amphibians, including clades of the microhylid genus *Stumpffia* and other *Gephyromantis*

clades have the highest species richness (Brown et al. 2016, Rakotoarison et al. 2017a).

Several aspects of our analyses will require future scrutiny from more extensive data sets. On the one hand, the phylogenetic relationships within the *G. plicifer* complex are not fully clarified; the more extensive combined mitochondrial data set (Fig. 3) placed *G. pedronoi* as sister to *G. luteus* whereas in the 16S tree (Fig. 1) it was recovered sister to *G. plicifer*. We consider the combined tree (Fig. 3) as more reliable as it is based on an almost five-fold higher number of nucleotides; yet the posterior probability of 0.93, below the 0.95 threshold, for the clade formed by *G. luteus* and *G. pedronoi* indicates that the deep nodes in the tree are not yet satisfyingly resolved. A further intriguing aspect is the large variation of the nuclear-encoded Rag-1 gene in *G. luteus*, compared to the few mutations separating it from *G. plicifer* and *G. pedronoi* (Fig. 4). This pattern may be explained by (a) the redefined *G. luteus* consisting of more than one species-level taxon as suggested by the high mitochondrial divergences among A1–A5, or (b) a

large effective population size as supported by the partly star-like arrangement of haplotypes, especially of A2–A5 (Fig. 4), or a combination of both.

Fully resolving the taxonomy of the *G. plicifer* complex, especially *G. luteus* (clade A), will require additional collections from contact zones and population genomic analyses, to understand the amount of gene flow among subclades A1–A5, as the steepness of possible hybrid zones of such apparently allopatric lineages provides a good indicator of species status (Dufresnes et al. 2021). Especially promising for this purpose is the Ankeniheny-Zahamena corridor, which still holds a largely continuous forested region linking populations of A4 and A2; and the area between Moramanga and Anosibe An'Ala, which should harbour the contact zone between A2 and A3. The areas between Anosibe An'Ala and Ranomafana (contact between A1 and A3) and the Masoala Peninsula and Anjanaharibe-Sud (possible contact between A4 and A5) would also be of interest, but logistically more difficult to sample. Finally, if there was a direct contact and maybe co-occurrence without admixture of A2 and A3 in the Andasibe/Maromizaha/An'Ala region, this could provide direct evidence for their species status. Ultimately, field surveys that comprise the collection of voucher specimens and samples for molecular analysis remain of high priority across Madagascar, but in well-surveyed areas should prioritize collecting specimens, including call vouchers, of taxonomically controversial taxa.

Acknowledgements

Assembling the many samples used in this work would not have been possible without the help of many colleagues, students and guides in the field; we are in particular grateful to P. Bora, E. Coppola, S. Hyde Roberts, P.-S. Gehring, M. Pabijan, D. Rakotomalala, F. Ranaivojoana, L. Randriamanana, R. D. Randrianiaina, J. E. Randrianirina, F. M. Ratsoavina, E. Rajeriarison T. Rajoafiarison, G. M. Rosa, and D. R. Vieites. M. Kondermann and G. Keunecke provided substantial assistance to laboratory work. L. Mashinini granted access to the collection of the Transvaal Museum in Pretoria. This work was carried out in framework of collaboration accords among the author's institutions, the Department of Animal Biology of the University of Antananarivo, and the Ministry of the Environment of the Republic of Madagascar. Various field campaigns were supported by the Volkswagen Foundation, Deutsche Forschungsgemeinschaft, Deutscher Akademischer Austauschdienst, Mohamed bin Zayed Species Conservation Fund, EDGE, Zoological Society of London, Amphibian Specialist Group, Saint Louis Zoo's Field Research for Conservation program (FRC# 16-09;

FRC# 12-12) of the Wildcare Institute, as well as the Portuguese National Funds through FCT – Fundação para a Ciência e a Tecnologia – support the 2020.00823. CEECIND contract for A. Crottini.

References

- Ahl, E. 1929. Beschreibung neuer Frösche aus Madagaskar. Mitteilungen aus dem Museum für Naturkunde in Berlin, Zoologische Reihe 14(3/4): 469–484.
- AmphibiaWeb 2021. Information on amphibian biology and conservation. AmphibiaWeb, Berkeley, California. Available from: <http://amphibiaweb.org/> [accessed 9 August 2021].
- Andreone, F., Vences, M., Glaw, F. & Randrianirina, J. E. 2007. Remarkable records of amphibians and reptiles on Madagascar's central high plateau. *Tropical Zoology* 20: 19–39.
- Avise, J. C. & Ball, R. M. 1990. Principles of genealogical concordance in species concepts and biological taxonomy. Pp. 45–67 in: Futuyma, D. & Antonovics, J. (eds). *Oxford surveys in evolutionary biology*. Oxford (Oxford Univ. Press).
- & Wollenberg, K. 1997. Phylogenetics and the origin of species. *Proceedings of the National Academy of Sciences of the USA* 94: 7748–7755.
- Basler, N., Xenikoudakis, G., Westbury, M. V., Song, L., Sheng, G. & Barlow, A. 2017. Reduction of the contaminant fraction of DNA obtained from an ancient giant panda bone. *BMC Research Notes* 10: 754.
- Blommers-Schlösser, R. M. A. 1979. *Biosystematics of the Malagasy frogs. I. Mantellinae (Ranidae)*. *Beaufortia* 352: 1–77.
- & Blanc, C. P. 1991. *Amphibiens (première partie). Faune de Madagascar* 75: 1–379.
- Bossuyt, F. & Milinkovitch, M. C. 2000. Convergent adaptive radiations in Madagascan and Asian ranid frogs reveal covariation between larval and adult traits. *Proceedings of the National Academy of Sciences of the USA* 97: 6585–6590.
- Boulenger, G. A. 1882. *Catalogue of the Batrachia Saliientia s. Ecaudata in the collection of the British Museum*. Second edition, London (Taylor and Francis).
- Boumans, L., Vieites, D. R., Glaw, F. & Vences, M. 2007. Geographical patterns of deep mitochondrial differentiation in widespread Malagasy reptiles. *Molecular Phylogenetics and Evolution* 45: 822–839.
- Brown, J. L., Sillero, N., Glaw, F., Bora, P., Vieites, D. R. & Vences, M. 2016. Spatial biodiversity patterns of Madagascar's amphibians and reptiles. *PLoS ONE* 11: e0144076.
- Dabney, J., Knapp, M., Glocke, I., Gansauge, M. T., Weihmann, A., Nickel, B., Valdiosera, C., García, N., Pääbo, S., Arsuaga, J. L. & Meyer, M. 2013. Complete mitochondrial genome sequence of a Middle Pleistocene cave bear reconstructed from ultrashort DNA fragments. *Proceedings of the National Academy of Sciences of the USA* 110: 15758–15763.

- de Queiroz, K. 1998. The general lineage concept of species, species criteria, and the process of speciation. Pp. 49–89 in: Howard, D. J. & Berlocher, S. H. (eds). *Endless forms. Species and speciation*. Oxford (Oxford University Press).
- 2007. Species concepts and species delimitation. *Systematic Biology* 56: 879–886.
- Dufresnes, C., Brelford, A., Jeffries, D. L., Mazepa, G., Suchan, T., Canestrelli, D., Nicieza, A., Fumagally, L., Dubey, S., Martinez-Solano, I., Litvinchuk, S. N., Vences, M., Perrin, N. & Crochet, P.-A. 2021. Master genes or mass of genes? A view on the genomic architecture of speciation from amphibian hybrid zones. *Proceedings of the National Academy of Sciences of the USA* 118: e2103963118.
- Folmer, O., Black, M., Hoeh, W., Lutz, R. & Vrijenhoek, R. 1994. DNA primers for amplification of mitochondrial cytochrome c oxidase subunit I from diverse metazoan invertebrates. *Molecular Marine Biotechnology* 3: 294–299.
- Frost, D. R. 2021. Amphibian species of the world: an online reference. Version 6.1 [accessed 01 September 2021] at <https://amphibiansoftheworld.amnh.org/index.php>. New York, USA (American Museum of Natural History).
- Gansauge, M.-T. & Meyer, M. 2013. Single-stranded DNA library preparation for the sequencing of ancient or damaged DNA. *Nature Methods* 8: 737–748.
- , Gerber, T., Glocke, I., Korlevic, P., Lippik, L., Nagel, S., Riehl, L. M., Schmidt, A. & Meyer, M. 2017. Single-stranded DNA library preparation from highly degraded DNA using T4 DNA ligase. *Nucleic Acids Research* 45: e79.
- Glaw, F. & Vences, M. 2006. Phylogeny and genus-level classification of mantellid frogs. *Organisms Diversity and Evolution* 6: 236–253.
- & Vences, M. 2007. *A field guide to the amphibians and reptiles of Madagascar*. Third edition, 496 pp., Cologne (Vences & Glaw Verlag).
- , Vences, M. & Gossmann, V. 2000. A new species of *Mantidactylus* from Madagascar, with a comparative survey of internal femoral gland structure in the genus (Amphibia: Ranidae: Mantellinae). *Journal of Natural History* 34: 1135–1154.
- Hrbek, T. & Larson, A. 1999. The evolution of diapause in the killifish family Rivulidae (Atherinomorpha, Cyprinodontiformes): a molecular phylogenetic and biogeographic perspective. *Evolution* 53: 1200–1216.
- IUCN 2012. *IUCN Red List categories and criteria: Version 3.1. 2nd edition*, Gland, Switzerland and Cambridge, UK (IUCN).
- IUCN SSC Amphibian Specialist Group 2016. *Boophis andohahela*. The IUCN Red List of Threatened Species 2016: e.T57388A68502153. <https://dx.doi.org/10.2305/IUCN.UK.2016-1.RLTS.T57388A68502153.en> [downloaded on 18 August 2021].
- Kaffenberger, N., Wollenberg, K. C., Köhler, J., Glaw, F., Vieites, D. R. & Vences, M. 2012. Molecular phylogeny and biogeography of Malagasy frogs of the genus *Gephyromantis*. *Molecular Phylogenetics and Evolution* 62: 555–560.
- Kocher, T. D., Thomas, W. K., Meyer, A., Edwards, S. V., Pääbo, S., Villablanca, F. X. & Wilson, A. C. 1989. Dynamics of mitochondrial DNA evolution in animals: amplification and sequencing with conserved primers. *Proceedings of the National Academy of Sciences of the USA* 86: 6196–6200.
- Köhler, J., Jansen, M., Rodríguez, A., Kok, P. J. R., Toledo, L. F., Emmrich, M., Glaw, F., Haddad, C. F. B., Rödel, M.-O. & Vences, M. 2017. The use of bioacoustics in anuran taxonomy: theory, terminology, methods and recommendations for best practice. *Zootaxa* 4251: 1–124.
- Kumar, S., Stecher, G., Li, M., Knyaz, C. & Tamura, K. 2018. MEGA X: Molecular Evolutionary Genetics Analysis across computing platforms. *Molecular Biology and Evolution* 35: 1547–1549.
- LANFEAR, R., CALCOTT, B., HO, S. Y. W. & GUINDON, S. 2012. PartitionFinder: combined selection of partitioning schemes and substitution models for phylogenetic analyses. *Molecular Biology and Evolution* 29: 1695–1701.
- Li, C., Corrigan, S., Yang, L., Straube, N., Harris, M., Hofreiter, M., White, W. T. & Naylor, G. J. P. 2015. DNA capture reveals transoceanic gene flow in endangered river sharks. *Proceedings of the National Academy of Sciences of the USA* 112: 13302–13307.
- Librado, P. & Rozas, J. 2009. DnaSP, Version 5. A software for comprehensive analysis of DNA polymorphism data. *Bioinformatics* 25: 1451–1452.
- Methuen, P. A. & Hewitt, J. 1913. On a collection of Batrachia from Madagascar made during the year 1911. *Annals of the Transvaal Museum, Pretoria* 4: 49–64 + 2 plates.
- Moat, J. & Smith, P. (eds) 2007. *Atlas of the vegetation of Madagascar*. 124 pp., Kew (Kew Publishing).
- Padial, J. M., Miralles, A., De la Riva, I. & Vences, M. 2010. The integrative future of taxonomy. *Frontiers in Zoology* 7: 16.
- Paijmans, J. L. A., Baleka, S., Henneberger, K., Taron, U. H., Trinks, A., Westbury, M. V. & Barlow, A. 2017. Sequencing single-stranded libraries on the Illumina NextSeq 500 platform. www.arXiv.org.arXiv:1711.11004.
- , Fickel, J., Courtiol, A., Hofreiter, M. & Förster, D. W. 2016. Impact of enrichment conditions on cross-species capture of fresh and degraded DNA. *Molecular Ecology Resources* 16: 42–55.
- Palumbi, S. R., Martin, A., Romano, S., McMillan, W. O., Stice, L. & Grabowski, G. 1991. *The Simple Fool's Guide to PCR*, Version 2.0. University of Hawaii (privately published).
- Pedrono, M. 2008. *The tortoises and turtles of Madagascar*. 147 pp., Kota Kinabalu, Malaysia (Natural History Publications (Borneo)).
- & Clausen, A. 2018. *Twilight of the Angonoka – biology and conservation of the World's rarest tortoise*. 184 pp., Kota Kinabalu, Malaysia (Natural History Publications (Borneo)).

- Perl, R. G. B., Nagy, Z. T., Sonet, G., Glaw, F., Wollenberg, K. C. & Vences, M. 2014. DNA barcoding Madagascar's amphibian fauna. *Amphibia-Reptilia* 35: 197–206.
- Rakotoarison, A., Scherz, M. D., Glaw, F., Köhler, J., Andreone, F., Franzen, M., Glos, J., Hawlitschek, O., Jono, T., Mori, A., Ndriantsoa, S. H., Rasoamampionona Raminosoa, N., Riemann, J. C., Rödel, M.-O., Rosa, G. M., Vieites, D. R., Crottini, A. & Vences, M. 2017a. Describing the smaller majority: integrative taxonomy reveals twenty-six new species of tiny microhylid frogs (genus *Stumpffia*) from Madagascar. *Vertebrate Zoology* 67: 271–398.
- , Scherz, M. D., Glaw, F. & Vences, M. 2017b. Rediscovery of frogs belonging to the enigmatic microhylid genus *Madecassophryne* in the Anosy Massif, south-eastern Madagascar. *Salamandra* 53: 507–518.
- Rancilhac, L., Bruy, T., Scherz, M. D., Almeida Pereira, E., Preick, M., Straube, N., Lyra, M. L., Ohler, A., Streicher, J. W., Andreone, F., Crottini, A., Hutter, C. R., Randrianantoandro, J. C., Rakotoarison, A., Glaw, F., Hofreiter, M. & Vences, M. 2020. Target-enriched DNA sequencing from historical type material enables a partial revision of the Madagascar giant stream frogs (genus *Mantidactylus*). *Journal of Natural History* 54: 87–118.
- Randrianiaina, R. D., Wollenberg, K. C., Rasolonjatovo Hiobiarilanto, T., Strauß, A., Glos, J. & Vences, M. 2011. Nidicolous tadpoles rather than direct development in Malagasy frogs of the genus *Gephyromantis*. *Journal of Natural History* 45: 2871–2900.
- Rohland, N., Siedel, H. & Hofreiter, M. 2004. Non-destructive DNA extraction method for mitochondrial DNA analyses of museum specimens. *Biotechniques* 36: 814–821.
- Ronquist, F., Teslenko, M., Van der Mark, P., Ayres, D. L., Darling, A., Höhna, S., Larget, B., Liu, L., Suchard, M. A. & Huelsenbeck, J. P. 2012. MrBayes 3.2: efficient Bayesian phylogenetic inference and model choice across a large model space. *Systematic Biology* 61: 539–542.
- Salzburger, W., Ewing, G. B. & Von Haeseler, A. 2011. The performance of phylogenetic algorithms in estimating haplotype genealogies with migration. *Molecular Ecology* 20: 1952–1963.
- Scherz, M. D., Razafindraibe, J. H., Rakotoarison, A., Bletz, M. C., Glaw, F. & Vences, M. 2017. Yet another small brown frog from high altitude on the Marojejy Massif, northeastern Madagascar. *Zootaxa* 4347: 572–582.
- , Rakotoarison, A., Ratsoavina, F. M., Hawlitschek, O., Vences, M. & Glaw, F. 2018. Two new Madagascar frog species of the *Gephyromantis* (*Duboisimantis*) *tandroka* complex from northern Madagascar. *Alytes* 36: 130–158.
- , Rasolonjatovo, S. M., Köhler, J., Rancilhac, L., Rakotoarison, A., Raselimanana, A. P., Ohler, A., Preick, M., Hofreiter, M., Glaw, F. & Vences, M. 2020. 'Barcode fishing' for archival DNA from historical type material overcomes taxonomic hurdles, enabling the description of a new frog species. *Scientific Reports* 10: 19109.
- Speybroeck, J., Beukema, W., Dufresnes, C., Fritz, U., Jablonski, D., Lymberakis, P., Martínez-Solano, I., Razzetti, E., Vamberger, M., Vences, M., Vörös, J. & Crochet, P.-A. 2020. Species list of the European herpetofauna – 2020 update by the Taxonomic Committee of the Societas Europaea Herpetologica. *Amphibia-Reptilia* 41: 139–189.
- Stephens, M., Smith, N. J. & Donnelly, P. 2001. A new statistical method for haplotype reconstruction from population data. *American Journal of Human Genetics* 68: 978–989.
- Straube, N., Lyra, M. L., Paijmans, J. L. A., Preick, M., Basler, N., Penner, J., Rödel, M.-O., Westbury, M. V., Haddad, C. F. B., Barlow, A. & Hofreiter, M. 2021. Successful application of ancient DNA extraction and library construction protocols to museum wet collection specimens. *Molecular Ecology Resources* 21(7): 2299–2315.
- Strauß, A., Randrianiaina, R. D., Vences, M. & Glos, J. 2013. Species distribution and assembly patterns of frog larvae in rainforest streams of Madagascar. *Hydrobiologia* 702: 27–43.
- Vences, M. & Glaw, F. 2001. Systematic review and molecular phylogenetic relationships of the direct developing Malagasy anurans of the *Mantidactylus asper* group (Amphibia, Mantellidae). *Alytes* 19: 107–139.
- , Glaw, F. & Márquez, R. 2006. The calls of the frogs of Madagascar. 3 Audio CDs and booklet, 44 pp., Barcelona (Alosa-Fonozoo).
- , Köhler, J., Pabijan, M., Bletz, M., Gehring, P.-S., Hawlitschek, O., Rakotoarison, A., Ratsoavina, F. M., Andreone, F., Crottini, A. & Glaw, F. 2017. Taxonomy and geographic distribution of Malagasy frogs of the *Gephyromantis asper* clade, with description of a new subgenus and revalidation of *Gephyromantis ceratophrys*. *Salamandra* 53: 77–98.
- , Kosuch, J., Glaw, F., Böhme, W. & Veith, M. 2003. Molecular phylogeny of hyperoliid treefrogs: biogeographic origin of Malagasy and Seychellean taxa and re-analysis of familial paraphyly. *Journal of Zoological Systematics and Evolutionary Research* 41: 205–215.
- , Miralles, A., Brouillet, S., Ducasse, J., Fedosov, A., Kharchev, V., Kostadinov, I., Kumari, S., Patmanidis, S., Scherz, M. D., Puillandre, N. & Renner, S. S. 2021. iTaxoTools 0.1: Kickstarting a specimen-based software toolkit for taxonomists. *Megataxa* 6: 77–92.
- Vieites, D. R., Wollenberg, K. C., Andreone, F., Köhler, J., Glaw, F. & Vences, M. 2009. Vast underestimation of Madagascar's biodiversity evidenced by an integrative amphibian inventory. *Proceedings of the National Academy of Sciences of the USA* 106: 8267–8272.

Appendix I: Detailed advertisement call descriptions of *Gephyromantis plicifer* and *G. luteus*

Gephyromantis luteus (Vevembe; subclade A1)

Advertisement calls of *Gephyromantis luteus* recorded on 9 February 2004, 18:20 h, at Vevembe (air temperature 23°C) consist of a short pulsed single note, emitted in series at regular intervals. Amplitude modulation is recognisable within calls, with maximum call energy being present at the middle of the calls' duration. Although partly masked by background sounds of insects, calls (= notes) seem to be clearly pulsed and in several calls 7–9 pulses are countable per note. Calls exhibit frequency modulation, namely an upward sweep in dominant frequencies. Numerical call parameters of 22 analysed calls are as follows (range followed by mean \pm standard deviation in parentheses): call duration (= note duration) 85–157 ms (111.9 \pm 19.7 ms); inter-call interval 195–253 ms (220.5 \pm 17.0 ms); call repetition rate within call series approximately 180 calls/minute; duration of call series 5745–5952 ms (n=2); number of calls per call series 18 (n=2); dominant frequency 3079–3660 Hz (3321 \pm 173 Hz), with a second peak of almost identical energy at around 1580–1670 Hz; prevalent bandwidth 1300–3800 Hz.

Gephyromantis luteus (Andasibe; possibly subclade A1, maybe A2 or A3)

Advertisement calls recorded on 12 January 1992 at Andasibe (air temperature 23°C; Vences et al. 2006, CD2, track 15, cut 3) agree in all general characteristics with the calls described above from Vevembe. Notes are clearly pulsed, with 6–10 pulses countable per note. Numerical call parameters of 18 analysed calls are as follows (range followed by mean \pm standard deviation in parentheses): call duration (= note duration) 93–147 ms (116.8 \pm 15.9 ms); inter-call interval 226–295 ms (272.3 \pm 28.9 ms); call repetition rate within call series approximately 150 calls/minute; duration of call series 5743 ms (n=1); number of calls per call series 15 (n=1); dominant frequency 3186–3294 Hz (3215 \pm 42 Hz); prevalent bandwidth 1300–5400 Hz.

Gephyromantis luteus (Ankeniheny; probably subclade A3 or maybe A2)

Advertisement calls of *Gephyromantis luteus* recorded on 20 February 1994, 19:30 h, at Ankeniheny (air temperature 21.6°C) consist of a short single note, emitted in series at regular intervals and fast succession. Amplitude modulation is recognisable within calls, with maximum call energy at the first two thirds

of the call's duration and then rapidly decreasing towards its end. No clear pulse structure is evident in the oscillograms, but to the human ear the note sounds somewhat 'noisy', not tonal. Calls exhibit frequency modulation, namely a slight upward sweep in dominant frequency. Numerical call parameters of 28 analysed calls are as follows (range followed by mean \pm standard deviation in parentheses): call duration (= note duration) 103–140 ms (114.5 \pm 13.5 ms); inter-call interval 184–238 ms (208.6 \pm 16.6 ms); call repetition rate within call series approximately 187 calls/minute; duration of call series 5931–7655 ms (n=3); number of calls per call series 19–26 (n=3); dominant frequency 3057–3402 Hz (3117 \pm 367 Hz); prevalent bandwidth 1400–4800 Hz.

Gephyromantis luteus (Nosy Boraha; subclade A4)

Advertisement calls of *Gephyromantis luteus* recorded in 20 February 1991, at Nosy Boraha (air temperature unknown) consist of a short single note, emitted in shorter series at somewhat irregular intervals. Amplitude modulation is recognisable within calls, with maximum call energy at the beginning of the call and then continuously decreasing towards its end. Notes are pulsatile in nature, although no clear pulse structure is evident from the oscillograms. Calls exhibit frequency modulation, namely a slight upward sweep in frequency. Numerical call parameters of 32 analysed calls are as follows (range followed by mean \pm standard deviation in parentheses): call duration (= note duration) 41–49 ms (43.3 \pm 2.8 ms); inter-call interval 144–379 ms (203.6 \pm 63.4 ms); call repetition rate within call series varies from 140–330 calls/minute; duration of call series 1122–2505 ms (n=4); number of calls per call series 6–12 (n=4); dominant frequency 3488–3811 Hz (3615 \pm 136 Hz), with a second peak of almost same energy at around 1630–1840 Hz; prevalent bandwidth 1300–4000 Hz.

Gephyromantis luteus (Marojejy; subclade A5)

Advertisement calls of *Gephyromantis luteus* recorded on 27 March 1994, 17:30 h, at Marojejy (air temperature 22.2°C) consist of a very short single note, emitted in series at regular intervals and fast succession. Amplitude modulation is recognisable within calls, with maximum call energy at the beginning of the call and slightly decreasing towards its end. No pulse structure is evident in the oscillograms, but to the human ear the note sounds somewhat 'noisy', not tonal. Calls exhibit frequency modulation, namely a slight upward sweep in dominant frequency. Numerical call parameters of 23 analysed calls are as follows (range followed by mean \pm standard deviation in parentheses): call duration

(= note duration) 18–35 ms (25.8 ± 5.6 ms); inter-call interval 159–191 ms (175.1 ± 10.0 ms); call repetition rate within call series approximately 290–300 calls/minute; duration of call series 2067–4086 ms ($n=2$); number of calls per call series 11–21 ($n=2$); dominant frequency 3337–3596 Hz (3350 ± 451 Hz); prevalent bandwidth 1400–7600 Hz.

***Gephyromantis plicifer* (Antoetra; clade B)**

Recordings of calls of *Gephyromantis plicifer* obtained on the 1st January and on the 30th January 2003 at Antoetra (17.5–18.0 °C air temperature) are slightly oversaturated in the recording level. This may mask part of the amplitude structure of calls, but the recording quality is good enough to characterise the call satisfactorily. The advertisement call consists of a single pulsatile note, usually emitted in series at regular intervals and rapid succession. There seems to be considerable amplitude modulation within each

call, with call energy being greatest at approximately the middle of the call's duration (energy peaks possibly cut by oversaturated recording level). The pulse structure is diffuse, with most pulses at least partly fused, except for the beginning of the calls where in most cases 4–8 pulses are countable. Call exhibit distinct frequency modulation, namely an upward frequency sweep with the dominant frequency starting at around 2400 Hz and increasing to around 3100 Hz towards the call's end. Numerical call parameters of 16 analysed calls are as follows (range followed by mean \pm standard deviation in parentheses): call duration (=note duration) 150–171 ms (161.0 ± 11.0 ms); inter-call interval 128–196 ms (148.1 ± 22.9 ms); call repetition rate within call series approximately 190 calls/minute; duration of call series 1776–2834 ms ($n=3$); number of calls per call series 5–9 ($n=3$); dominant frequency 2897–3127 Hz (2987 ± 65 Hz), with a second weaker peak at around 8400–9500 Hz; prevalent bandwidth 1100–5000 Hz.